

NEW ANIDOLIC PARAMETRIC TROUGHS CONCENTRATORS FOR SOLAR THERMAL ENERGY POWER PLANTS

CAPTADOR ANIDÓLICO DE CANAL PARAMÉTRICO PARA CENTRAL TERMOSOLAR

**A thesis submitted to the Department of Energy
Engineering of the University of Seville, in fulfillment
of the requirements for the degree of Doctor of
Philosophy**

Author: Juan Pablo Nuñez Bootello
Seville, Dic 2015

Supervisors:
Dr. Manuel Doblaré Castellano
Dr. Manuel Silva Pérez

Don MANUEL DOBLARÉ CASTELLANO, con DNI 30425335-S, Catedrático del Departamento de Ingeniería Mecánica de la Universidad de Zaragoza y Don MANUEL A. SILVA PÉREZ con DNI 28538050H, Profesor Contratado Doctor del Departamento de Ingeniería Energética de la Universidad de Sevilla,

HACEN CONSTAR:

que D. JUAN PABLO NÚÑEZ BOOTELLO, Ingeniero Industrial especialidad Mecánica y Master en Sistemas de Energía Térmica ha realizado bajo su dirección la presente memoria de tesis doctoral titulada :

“NEW ANIDOLIC PARAMETRIC TROUGHS CONCENTRATORS FOR SOLAR THERMAL ENERGY POWER PLANTS”

“CAPTADOR ANIDÓLICO DE CANAL PARAMÉTRICO PARA CENTRAL TERMOSOLAR”

Con esta fecha autorizan su presentación para optar al título de doctor

Sevilla, Diciembre de 2015

Fdo: Manuel A Silva Pérez y Manuel Doblaré Castellano

ACKNOWLEDGEMENTS

This thesis is the culmination of a dream

I would like to express my gratitude to my supervisors, Professor Manuel Doblaré and Doctor Manuel Silva for their guidance, advice, understanding and considerations on my work.

Special and deepest thankfulness to Manuel Doblaré for his generosity and for the confidence he has shown in me from the beginning.

I owe many thanks to my company Abengoa that gave me the opportunity to discover the world of renewable energies and to be part of a team at the forefront in research and technological development on its related topics. I particularize this acknowledgement in Hank Price, Markus Schramm and Monica de Mier for their technical support, but also in all the colleagues with whom I have had the chance to work with and that have supported or influenced the development of this work. In that regards, my special thanks go to Antonio Esteban.

I wish to express my gratitude also to Professor M. Lourdes Garcia Rodriguez for her valuable advice.

People who have had the chance to be born in stability and “abundance” have the duty to learn and study to transform our society to a better one, and to transmit this knowledge to our children, and encourage them to learn in love and respect to others and in a collective commitment to action.

I dedicate this thesis to my wife Carmen and my three daughters Carmen, Ana and Mercedes.

CONTENTS

ACKNOWLEDGEMENTS	5
CONTENTS	7
RESUMEN	9
PUBLICATIONS	19
LIST OF FIGURES.....	21
LIST OF TABLES.....	23
LIST OF SYMBOLS	25
INTRODUCTION.....	27
OBJECTIVES.....	31
1. CHAPTER 1: EXERGY OF THE SUN RADIATION	33
1.1 Fundamental expressions for the energy and entropy of the sun radiation	34
1.1.1 Planck's Blackbody Formulas	35
1.1.2 The sun as a blackbody radiator.	38
1.2 Maximum possible useful work from sun radiation	45
2. CHAPTER 2: SOLAR CONCENTRATORS. ETENDUE AND MAXIMUM CONCENTRATION 51	
2.1 The concept of etendue	52
2.1.1 Conservation of etendue.....	52
2.1.2 Imperfect optical systems	55
2.2 Maximum <i>concentration</i> that a solar concentrator can provide	56
3. CHAPTER 3: OPTICAL ANALYSIS OF A TWO STAGE XX SIMULTANEOUS MULTIPLE SURFACE (SMS) CONCENTRATOR FOR PARAMETRIC TROUGH PRIMARY AND FLAT ABSORBER WITH APPLICATION IN DIRECT STEAM GENERATION (DSG) SOLAR THERMAL PLANTS	61
4. CHAPTER 4: OPTICAL ANALYSIS OF A TWO STAGE XX CONCENTRATOR FOR PARAMETRIC TROUGH PRIMARY AND TUBULAR ABSORBER WITH APPLICATION IN SOLAR THERMAL ENERGY (STE) TROUGH POWER PLANTS	63
5. CHAPTER 5: PARABOLIC TROUGHS vs FRESNEL CONCENTRATORS.....	65
6. CHAPTER 6: AERODYNAMICS OF NEW SOLAR PARAMETRIC TROUGHS: TWO DIMENSIONAL AND THREE DIEMENSIONAL SINGLE MODULE NUMERICAL ANALYSIS	67
7. CHAPTER 7: PARAMETRIC TROUGH COLLECTOR (PmTC) FOR A COMMERCIAL EVACUATED RECEIVER: OPTICAL PERFORMANCE AND PLANT SIMULATIONS	71
CONCLUSIONS.....	75
Main contributions.....	77

Future Work.....	78
8. ANNEX 1: COMMENTS ON THE CONVERSION OF ENCLOSED BLACKBODY RADIATION 79	
9. ANNEXE 2: PTC DEVELOPMENTS IN ABENGOA IN THE LAST 15 YEARS	83
REFERENCES.....	87

RESUMEN

Es un hecho que las centrales de producción de energía eléctrica a partir de energía solar pueden proporcionar energía segura con costos futuros previsibles, en gran parte no afectados por la geopolítica y los mercados mundiales de la energía (International Energy Agency, 2007). Sin embargo, el aprovechamiento de la radiación solar de manera eficiente para la generación de electricidad es todavía un reto (International Energy Agency, 2014).

Las centrales de captadores de canal parabólico constituyen la tecnología solar térmica más madura en comparación con la tecnología de receptor central de torre y la de captadores Fresnel. Prueba de ello es que, desde la entrada en operación de las centrales SEGS en California en los años 80, más de 2 GW de esta tecnología se han puesto en operación en todo el mundo (CSP World Map)

Aunque este tipo de centrales no son a día de hoy competitivas en coste de electricidad frente a las centrales de combustible fósil, tienen un gran margen de mejora tanto en aumento en eficiencia como en reducción de costes que podría permitir reducir e incluso anular esta diferencia (International Energy Agency, 2014). El desarrollo de la generación directa de vapor o el uso de sales fundidas como fluidos de transferencia de calor suponen un avance importante por cuanto dejan de utilizarse aceites térmicos limitados en temperatura y es posible aumentar la eficiencia del ciclo termodinámico (Zarza E., 2004, Estela, 2012). Desde el punto de vista óptico, la geometría parabólica está lejos del límite termodinámico de concentración y puede ser optimizada para incrementar la captación de radiación solar por metro de tubo absorbedor (International Energy Agency, 2014), algo que ya se está consiguiendo con los captadores tipo Fresnel (Collares M., 2009). En el caso de los captadores de canal parabólico, sin embargo, el desafío es hacerlo sin penalizar los costes estructurales por una mayor distancia del receptor a los espejos primarios o por cargas de viento mayores, y de manera que se pueda aumentar la temperatura de operación y la eficiencia del ciclo de Rankine reduciendo comparativamente las pérdidas térmicas del tubo absorbedor a la atmósfera (International Energy Agency, 2014).

En este sentido la Óptica Anidólica o no formadora de imagen, desarrollada en los años 80 por Welford y Winston (Welford W. T., 1989), es una herramienta muy potente utilizada en el diseño de captadores solares. Durante las tres últimas décadas esta rama de la Óptica Geométrica ha sufrido una evolución importante que se ha traducido en la progresiva evolución y optimización, sobre todo, de captadores fotovoltaicos de concentración.

En lo que se refiere a los captadores de canal parabólico se han realizado distintos intentos para optimizar su rendimiento manteniendo la sección parabólica de la que toman su nombre (Rabl A., 1982). Estos desarrollos se han centrado principalmente en optimizar la concentración mejorando el apunte, reduciendo las deformadas estructurales y los errores de fabricación y montaje. Independientemente de los esfuerzos que se pueden seguir haciendo en esta dirección, la relación de concentración de los captadores de canal parabólico frente a la concentración máxima teóricamente alcanzable para estas geometrías se mantiene constante si no se modifica el ángulo de borde, lo que sólo es posible mediante el uso de concentradores secundarios y nuevas geometrías ópticas (Pereira M.C., 1991)

Dentro de la óptica anidólica, y en esta línea, se han realizado diseños de concentradores secundarios ((Ciemat, 1990 y Collares M., 1991) que han resultado en geometrías más o menos complejas que, o bien necesitan estar en contacto con el tubo absorbedor - lo cual resulta poco práctico puesto que el tubo absorbedor de este tipo de centrales necesariamente debe llevar vacío para no penalizar excesivamente las pérdidas térmicas globales por unidad de longitud - o bien alejan el conjunto secundario receptor del primario, lo cual penaliza estructuralmente los diseños de los soportes haciendo que resulte más práctico reorientar el diseño a un captador de tipo Fresnel en el que el absorbedor y el secundario quedan desvinculados del primario.

Adicionalmente se han planteado diseños en los que el primario deja de ser una parábola para convertirse en una curva paramétrica y en los que el concentrador secundario no toca el tubo absorbedor (Benítez P., 1997 y Cannavaro D., 2013). Este tipo de colectores ha sido bautizado por los autores de esta tesis como captadores de canal paramétrico.

Es en esta última línea en la que se plantea la presente tesis doctoral. En ella se investiga la utilización de la óptica anidólica para la obtención de captadores de radiación solar de tipo canal paramétrico que sean más eficientes ópticamente, térmicamente y estructuralmente, y que permitan aumentar la eficiencia global de las plantas termosolares de concentración.

La memoria de la tesis queda así estructurada en 7 capítulos:

El primer capítulo se centra en la descripción termodinámica de la radiación solar que llega a la tierra y en una discusión inicial sobre el trabajo útil máximo que se puede

obtener de la misma, como paso previo al análisis de su límite en concentración y como introducción necesaria para entender bien el concepto de etendue.

En el capítulo dos se introduce la etendue y se aborda el principio de su conservación. Ambas cuestiones constituyen la base de la óptica anidólica y dos pilares fundamentales sobre los que se apoya el resto de la tesis. El capítulo concluye definiendo el límite físico en concentración de la radiación solar. Este límite será utilizado, a posteriori, como referencia para definir dónde están los captadores del estado del arte y cuál es el potencial de mejora siempre desde un punto de vista de la concentración.

En el capítulo tres se realiza una revisión de la óptica de los captadores de canal parabólico. Es en este capítulo donde se propone un nuevo captador ya de geometría paramétrica – no parabólica – para generación directa de vapor y con óptica optimizada para receptor plano multitubular similar al utilizado en el Compact Linear Fresnel Concentrator (CLFC) desarrollado y construido por Mills en los primeros años del presente siglo (Mills D.R., 2000). En el capítulo se explica el método de diseño y las condiciones de contorno utilizadas en los cálculos. El captador propuesto incluye el mencionado receptor multitubular con cerramiento transparente sin vacío y, adicionalmente, mantiene ángulos de borde elevados y añade flexibilidad geométrica con potencial de mejora aerodinámico. En la última parte se realiza una comparación de la óptica con los captadores de canal parabólico y de canal paramétrico en el estado del arte.

En el capítulo cuatro se propone otro nuevo captador también de geometría paramétrica pero con óptica optimizada para receptor circular. El captador se puede utilizar tanto para generación directa de vapor como en plantas termosolares con aceite o sales como fluidos caloportadores. En el capítulo se explica el método de diseño y las condiciones de contorno utilizadas en los cálculos y se hace un análisis paramétrico detallado jugando con las mismas. El diseño propuesto deja abierta la posibilidad de utilizar un receptor comercial con vacío y un secundario externo, o un receptor no comercial con tubo absorbedor comercial y con tubo de vidrio excéntrico de mayor diámetro al comercial y parcialmente espejado. La nueva geometría mantiene también ángulos de borde elevados y añade flexibilidad geométrica con potencial de mejora aerodinámico. En la última parte se realiza, como en el capítulo anterior, una comparación de la óptica con los captadores de canal parabólico y de canal paramétrico en el estado del arte.

Aunque no es el objeto de esta tesis comparar el potencial de las plantas de captadores tipo Fresnel con la de los captadores de canal parabólico y/o paramétrico, en el capítulo

cinco se estudia la óptica de los captadores tipo Fresnel que están en el estado del arte en términos de concentración relativa a concentración máxima. Puesto que ambos tipos de captadores comparten el mismo límite de concentración es importante analizar el potencial óptico de cada uno por separado y compararlos entre sí, aunque entender cuál de los dos conceptos tiene más potencial desde un punto de vista de planta requiere, por las características específicas de cada uno, analizar en detalle las pérdidas por efecto coseno, la geometría del receptor y sus pérdidas térmicas, y la configuración de planta incluyendo los costes de los diferentes componentes.

En el capítulo seis se presentan los resultados de ensayos de túnel de viento virtuales usando herramientas de simulación CFD (Computational Fluid dynamics) sobre módulos aislados. El objetivo es entender los campos de velocidades y las cargas de viento generadas en los dos captadores cilindro paramétricos propuestos en comparativo entre ellos y también en comparativo con los de canal parabólico del estado del arte (LS2 y LS3 / Eurotrough). Una batería de simulaciones bidimensionales y tridimensionales permite concluir que el captador de canal paramétrico para receptor plano se comporta peor que el captador de canal paramétrico para receptor circular en lo referente a cargas de viento. Este inconveniente, añadido al hecho de que en este captador todos los rayos sufren doble reflexión – en el caso del captador paramétrico para receptor circular sólo un 15% de los rayos sufren doble reflexión – y al hecho de que no existe una solución comercial para el receptor multitubular propuesto, han inducido al autor a seleccionar el captador de canal paramétrico para receptor tubular comercial con vacío como la opción a evaluar a nivel de planta en comparativo con la tecnología actual.

En el capítulo siete se realiza esta evaluación. En primer lugar se genera un modelo de una planta comercial de 50 MWe sin almacenamiento y con aceite como fluido caloportador en la ciudad de Sevilla. Adicionalmente se desarrolla un segundo modelo con el captador de canal paramétrico para receptor circular comercial seleccionado, con área análoga de colector y mismo flujo máscio por lazo. Puesto que en el proceso de diseño de los captadores anidólicos se supone comportamiento ideal y se ignoran las pérdidas por transmisión, absorción y reflexión, en este capítulo se realizan trazados de rayos tipo Montecarlo con distribuciones de errores reales tomadas de prototipos de apertura y geometría similares e incluyendo la interacción luz – materia. Para realizar la comparación final se lanzan simulaciones anuales y se desglosan las pérdidas térmicas y la producción eléctrica de ambas plantas

Objetivos

Existen dos líneas de trabajo que, desde un punto de la investigación, el desarrollo y la innovación, están tratando de mejorar la tecnología actual en el campo solar de las plantas de captadores de canal parabólico. Por un lado se están desarrollando captadores parabólicos cada vez más precisos y con menos tolerancias de fabricación y errores de montaje. Pese a que esta línea de trabajo mantiene la ratio concentración a concentración máxima inalterado, permite mejorar la concentración a costa de reducir la aceptancia angular del captador. La otra tendencia va orientada a impulsar el desarrollo de captadores anidólicos (o no formadores de imagen). Esta línea permite aumentar la ratio concentración a concentración máxima de manera efectiva o, lo que es lo mismo, permite mejorar la concentración manteniendo la aceptancia angular de los captadores en sus niveles actuales y sin penalizar inversión en mejorar la precisión del seguimiento y las tolerancias de fabricación y de montaje.

En este marco, el objetivo principal de esta tesis ha sido la búsqueda de nuevas geometrías de captadores de canal paramétrico obtenidos mediante óptica anidólica que permitan mejorar la eficiencia óptica, térmica y estructural en comparación a los captadores actuales de canal parabólico permitiendo así incrementar de manera más eficiente la temperatura de operación y mejorar la eficiencia global de las plantas termosolares basadas en esta tecnología.

Desde el punto de vista estructural, el uso de metodologías de diseños ópticos que permitan reducir las cargas de viento con huecos en los espejos o controlando la separación absorbedor – reflector pueden ayudar no sólo a mejorar la eficiencia sino también a reducir el coste. Puesto que la estructura está estrechamente ligada a la óptica y viceversa, la óptica anidólica añade una evidente flexibilidad en esta dirección.

Con todo ello, en base a la propia experiencia y a la profunda revisión bibliográfica realizada en captadores de canal parabólico y en captadores tipo Fresnel, se plantean como objetivos específicos de esta tesis los siguientes:

- i) obtener una mejora óptica importante acercando la ratio concentración frente a concentración máxima lo más posible al límite termodinámico en comparación con el captador LS3 / Eurotrough y minimizando el porcentaje de rayos que se reflejan en el concentrador secundario frente al total de rayos captados por el primario,
- ii) añadir flexibilidad geométrica en el diseño orientada a reducir los costes estructurales reduciendo las cargas de viento por un lado, y por otro lado

minimizando la distancia del primario al conjunto secundario - absorbedor con ángulos de borde lo más cercano posible a 90º,

iii) evaluar el potencial de las propuestas proyectando las soluciones en planta comercial.

Contexto

Los trabajos llevados a cabo en esta tesis doctoral se desarrollan en un doble contexto:

- Dentro de una vertiente académica y universitaria, el doctorando es Ingeniero Industrial Mecánico de formación por la Universidad de Sevilla (plan de estudios aprobado por Orden Ministerial de 30 de Julio de 1975), posee la titulación de Project Manager Program (2011, Georgetown University, EEUU) y ha cumplimentado el Master Universitario en Sistemas de Energía Térmica por la Universidad de Sevilla en Septiembre de 2013. Adicionalmente desde el 24 de Marzo de 2014 el doctorando es Asistente Honorario del Departamento de Ingeniería Energética de la Universidad de Sevilla.

- Por otro lado, el doctorando es actualmente director de innovación y consultoría avanzada en Abengoa Research y cuenta con más de quince años de experiencia profesional como responsable de I+D+i en distintas empresas y sectores. El doctorando empezó con una Beca Aicia en el departamento de Elasticidad y Resistencia de Materiales de la Universidad de Sevilla trabajando con elementos de contorno aplicados a materiales anisótropos funcionalmente graduados. Posteriormente trabajó 2 años como Ingeniero Mecánico en el sector aero especial para las compañías Arianspace & Cnes realizando simulaciones mecánicas de configuraciones de vuelo de las lanzaderas Ariane 4 y Ariane 5. Después trabajó 5 años en el sector de la automoción como Ingeniero de I+D en la compañía Valeo como responsable de diseño mecánico ante vibraciones y a impacto a baja velocidad de los frontales de los vehículos. Finalmente, en el año 2008, se unió a Abengoa como director de investigación y desarrollo y responsable de diferentes proyectos nacionales e internacionales relacionados con la energía solar de concentración. Desde 2013 a principios de 2015 fue también director del área termosolar en Abengoa Research.

Conclusiones

Las principales conclusiones de esta tesis son:

1. Se proponen dos captadores de canal paramétrico, uno para receptor multitubular plano con cerramiento transparente sin vacío plano, y otro para receptor circular comercial con vacío y un secundario externo, o para receptor no comercial con tubo absorbedor comercial y con tubo de vidrio excéntrico de mayor diámetro al comercial y parcialmente espejado. El primero aplica para generación directa de vapor mientras que el segundo aplica tanto para generación directa de vapor como para plantas termosolares con aceite o sales como fluidos caloportadores
2. Se realiza una comparación de los captadores propuestos con los captadores de canal parabólico y de tipo Fresnel del estado del arte en términos de concentración relativa a concentración máxima. La comparación con los captadores LS3 / Eurotrough muestra mejoras del 90% para aceptancias similares. Las geometrías propuestas mantienen ángulos de borde superiores a 80º y añaden flexibilidad geométrica con potencial de mejora aerodinámico gracias a la discontinuidad en los respectivos primarios. La comparación con los captadores tipo Fresnel se hace únicamente desde un punto de vista óptico porque ambos tipos de captadores comparten el mismo límite de concentración. Queda fuera del alcance de esta tesis realizar la comparación a nivel de planta. De esta manera el captador Fresnel de mayor eficiencia óptica es el “etendue-matched” con un producto eficiencia x concentración relativa a concentración máxima en el intervalo 55% a 85% que es mayor que el 60% obtenido con el mejor captador paramétrico de los dos que se proponen.
3. Las simulaciones fluido dinámicas sobre módulos aislados confirman que la solución para receptor circular se comporta de manera muy parecida a los captadores LS3 / Eurotrough para los coeficientes de resistencia, sustentación y momento. Por el contrario, la solución para receptor plano muestra una penalización superior al 25% en resistencia y momento máximos, y superior el 50% en sustentación máxima. Estos resultados sumados al hecho de que los rayos sufren dos reflexiones antes de llegar al receptor (en el caso del captador para receptor circular sólo el 15% de los rayos sufren doble reflexión), y al hecho de que no existe una solución comercial para la geometría de receptor multitubular propuesta motivan la elección del captador paramétrico para receptor circular como la opción a estudiar a nivel de planta.
4. Se generan dos modelos de planta comercial de 50 MWe sin almacenamiento y con aceite como fluido caloportador en la ciudad de Sevilla: uno con el captador LS3 / Eurotrough y otro con el captador paramétrico seleccionado; ambos con similar área de captación por colector y el mismo flujo másico por lazo. Puesto que en el proceso

de diseño de los captadores anidólicos se supuso comportamiento ideal y se ignoraron las pérdidas por transmisión, absorción y reflexión, se realizan simulaciones ópticas de trazado de rayos tipo Montecarlo con distribuciones de errores reales e incluyendo pérdidas por reflexión de Fresnel. Contrariamente a lo esperado la planta con los nuevos captadores penaliza la eficiencia óptica un 5.1% debido a la penalización por reflectividad y posible ensuciamiento del secundario, a un aumento de las pérdidas por final de colector y a las pérdidas por reflexión de Fresnel en el tubo absorbedor. Aunque el aumento de la concentración genera unas pérdidas térmicas del receptor al ambiente menores, la producción de electricidad se penaliza en un 2.5%. Con todo ello se concluye que la solución propuesta no mejora el estado del arte a nivel de planta para una temperatura nominal de salida de lazo del fluido caloportador de 391°C.

Aportaciones de la tesis

La contribución fundamental del presente trabajo ha sido avanzar en el entendimiento y en la evaluación del potencial de la óptica anidólica para generar nuevas geometrías de captadores que mejoren la eficiencia global y maximicen la producción de electricidad de las plantas termosolares de concentración.

De manera específica las aportaciones de la tesis son:

1. Propuesta de un nuevo captador de geometría paramétrica con óptica optimizada para receptor plano multitubular, con ángulos de borde elevados y con potencial de mejora aerodinámico.
2. Desarrollo de un nuevo método de diseño óptico y propuesta de un nuevo captador de geometría paramétrica con óptica optimizada para receptor circular que minimiza el porcentaje de rayos que pasan por el concentrador secundario frente al total de rayos captados por el primario, con ángulos de borde elevados, con potencial de mejora aerodinámico y con la posibilidad de utilizar un receptor absorbedor comercial.
3. Comparativa a nivel de ratio concentración a concentración máxima del estado del arte de los captadores de canal parabólico y Fresnel.
4. Caracterización del comportamiento ante carga de viento de los captadores propuestos.
5. Proyección del comportamiento real de los captadores propuestos mediante trazado de rayos tipo Montecarlo con distribuciones de errores reales tomadas de prototipos de apertura y geometría similares e incluyendo pérdidas por reflexión de Fresnel.

6. Elaboración de un modelo de planta, cálculo de las pérdidas térmicas del campo solar con el nuevo captador y estudio de la producción de energía anual así como comparación con planta de captadores comerciales de la misma potencia nominal

PUBLICATIONS

The following journal papers accompany this research:

Nunez-Bootello J.P., Price H., Silva Perez M., Doblare M., 2016 (accepted for publication), Optical analysis of a two stage xx SMS concentrator for parametric trough primary and flat absorber with application in DSG solar thermal plants. ASME Solar Energy Engineering: Including Wind Energy and Building Energy Conservation

Nunez-Bootello J.P., Price H., Silva Perez M., Doblare M., (under review), Optical analysis of a two stage xx concentrator for parametric trough primary and tubular absorber with application in STE trough solar plants. ASME Solar Energy Engineering: Including Wind Energy and Building Energy Conservation

Aerodynamics of new solar parametric troughs: two dimensional and three dimensional single module numerical analysis (under writing)

Parametric trough collector (pmtc) for a commercial evacuated receiver: optical performance and plant simulations (under writing)

LIST OF FIGURES

Figure 1-1 Solar Spectrum	35
Figure 1-2 The solid angle subtended by dA_n at a point on dA_1 (Incropera F.P., 2007)	39
Figure 1-3 The projection of dA_1 normal to the direction of radiation (Incropera F.P., 2007)	39
Figure 1-4 Emission from a differential element of area dA_1 into a hemisphere centered on dA_1 (Incropera F.P., 2007).....	40
Figure 1-5 Particle emitting in the sphere	41
Figure 1-6 Black body (unpolarized) radiation – Power scheme	43
Figure 1-7 Black body (unpolarized) radiation – Entropy scheme	44
Figure 1-8 Light emitted by the sun that reaches the earth confined within a cone of angle 2δ . Entropy rate and the power irradiance balance.....	45
Figure 1-9 Enclosure with perfectly reflecting internal surfaces (Bejan A., 2006).....	47
Figure 1-10 Reversible and adiabatic expansion for calculating the non flow exergy of enclosed blackbody radiation (Bejan A., 2006)	48
Figure 2-1 Interior of a box illuminated with three flashlights with small angular spread (Chaves J., 2008)	53
Figure 2-2 Interior of a box illuminated with three flashlights with large angular spread (Chaves J., 2008)	53
Figure 2-3 3D case: The etendue of the light emitted by dA_1 toward dA_2 equals that of light emitted	54
Figure 2-4 2D case: The etendue of the light emitted by da_1 toward da_2 equals that of light emitted	55
Figure 2-5 Loss of light and etendue in a system that conserves radiance (Chaves J., 2008)	56
Figure 2-6 Radiance decrease when light travels in an absorptive optical system (Chaves J., 2008)	56
Figure 2-7 Etendue in two and three dimensions (normal incidence).....	56
Figure 2-8 A two dimensional optical device with an entrance aperture a_1 and exit aperture a_2 . At the entrance aperture, the refractive index is n_1 and the half-angular aperture of the radiation is δ_1 . At the exit aperture, the refractive index is n_2 and the half-angular aperture of the radiation is δ_2 (Chaves J., 2008)	58
Figure 2-9 A three dimensional optical device with an entrance aperture A_1 and exit aperture A_2 . At the entrance aperture, the refractive index is n_1 and the half-angular aperture of the radiation is δ_1 . At the exit aperture, the refractive index is n_2 and the half-angular aperture of the radiation is δ_2 (Chaves J., 2008)	58
Figure 8-1 Reversible cycle executed by an enclosed radiation system in communication with two temperature reservoirs (Bejan A., 2006)	79

Figure 9-1 Eurotrough Collector	83
Figure 9-2 Abengoa Astro Collector	83
Figure 9-3 Abengoa Phoenix Gen 2.0 Collector	84
Figure 9-4 Abengoa E 2 Collector	84
Figure 9-5 Abengoa SpacetTube Collector	84

LIST OF TABLES

No se encuentran elementos de tabla de ilustraciones.

LIST OF SYMBOLS

δ	Half-acceptance angle of the concentrator
C	Geometric Concentration
C_{max}	Thermodynamic maximum concentration that can be achieved
f	Angle Transmission Curve
U	Etendue
ν	Frequency
P	Degree of polarization
h	Planck's constant
c	Speed of light
k	Boltzman's constant
σ	Steffan-Boltzman constant
Ω	Solid angle (sr)
A	Area
V	Volume
n	Refractive index
E	Energy
$K_{\nu,b}$	Blackbody spectral energy radiance
K_b	Blackbody energy radiance
Φ_b	Blackbody power
U	Energy emitted per unit volume
N	Rate of photons emitted per unit area and time
n	Rate of photons emitted per unit volume
I	Intensity of the radiation field
$L_{\nu,b}$	Blackbody spectral entropy radiance
L_b	Blackbody entropy radiance
Ψ_b	Blackbody entropy rate
S	Entropy emitted per unit volume
μ	Chemical potential
CEC	Compound Elliptical Concentrator
CFD	Computational Fluid Dynamics
CLFR	Compact Linear Fresnel Reflector
CPC	Compound Parabolic Concentrator
CRS	Central Receiver System
CSP	Concentrated Solar Power
DSG	Direct Steam Generation
LCoE	Levelized Cost of Electricity
IAM	Incidence Angel Modifier
IEA	International Energy Agency
NREL	National Renewable Energy Laboratory

PTC	Parabolic Trough Collector
PmTC	Parametric Trough Collector
SAM	System Advisor Model
SCA	Solar Collector Assembly
SEGS	Solar Electric Generating Systems plants
SMS	Simultaneous Multiple Surface
TERC	Tailored Edge Ray Concentrators
T	Temperature
XX	Reflective plus reflective optic

INTRODUCTION

It is a fact that plants producing electricity from solar energy can provide safe energy with predictable costs unaffected by geopolitics and global energy markets constraints (International Energy Agency, 2007). However, the use of solar radiation to generate electricity in a cost effective way remains still a challenge (International Energy Agency, 2014). Current Parabolic Trough Collector (PTC) technology is the most mature technology when compared to Central Receiver (CRS) and Fresnel systems. Since the first Solar Electric Generating Systems (SEGS) plants built in the Mojave Desert in California in the 80's using the LS-2 and LS-3 generations of PTCs that marked the beginning of modern development of Concentrated Solar Power (CSP) plants worldwide (Fernández-García A., 2010), today more than 2GW of this technology are currently on operation worldwide (CSP World Map, 2015).

Even if solar thermal energy power plants are not yet competitive in terms of cost of electricity when compared to fossil fuel plants, there is enough room for improvements, in both efficiency and costs, to reduce or even eliminate this gap (International Energy Agency, 2014). The use of molten salt and water as heat transfer fluids instead of oil allows achieving more efficient plants (Zarza E., 2004, Estela, 2012). From an optical point of view parabolic trough collectors optics is far from the thermodynamic limit and there is room to bring the concentration closer to the physical limit (International Energy Agency, 2014) – as it is currently been done with the Fresnel collectors (Collares M., 2009) – and to increase the operating temperature and the cycle efficiency while comparatively reducing heat losses to the atmosphere and reducing wind loads and receiver distance to the mirrors to minimize structural costs.

In that regards non-imaging optics (also called anidolic optics), developed in the 80's by Welford and Winston (Welford W. T., 1989), is a powerful tool used in the development of solar concentrators. During the last three decades this branch of the Geometrical Optics has undergone a major evolution that has resulted in the progressive development and optimization of, mainly, photovoltaic concentrators.

Regarding PTCs there have been some attempts to optimize its optics maintaining the parabolic shape (Rabl A., 1982). Some developments focus in increasing the concentration trough a reduction in the acceptance angle, which places a higher demand in tracking accuracy and reduces tolerances with respect to wind loads, quality of mirrors, control and mounting imprecisions. With this strategy, even if the concentration is improved, the ratio concentration relative to the thermodynamic

maximum limit remains constant if the rim angle is not changed. In fact, this value can only be modified using secondary concentrators or new optical geometries. There exist proposals improving the PTC performance by means of secondary concentrators sometimes with complex shapes and, in other cases, with secondary mirrors in contact with or very close to the absorber tube (Ciemat, 1990, Collares M., 1991). These solutions force designers to locate the secondary inside the evacuated tube, which is unpractical from a manufacturing point of view. There exist other proposals that use commercial evacuated tubes and accommodate the gap between the glass envelope and the receiver tube without losses being compatible with the placement of second stage mirrors outside the glass envelope but generating a large separation of the receiver to the primary reflector (Rabl A., 1985). This approach penalises the concentrator in terms of structural cost so that it is more practical to reorient the design towards a Fresnel type concentrator where both the absorber and the secondary remain mechanically independent of the primary.

Other non-parabolic primary mirrors solutions have been proposed with a sizeable gap between the optics and the absorber (Benitez P., 1997, Cannavaro D., 2013). In this case the proposed primary curve is no longer a parabola. In order to make the distinction with the traditional parabolic shape and taking into account that the new curve is a parametric one authors have decided to use this name in this work.

It is from this point that the motivation for the present work arises. In this thesis the use of anidolic optics to obtain parametric trough concentrators with improved optical, thermal and structural efficiency is investigated and compared to current parabolic trough solutions with the aim of increasing the overall efficiency of current solar thermal power plants.

The present document is structured in 7 chapters:

In chapter one a thermodynamic description of the solar radiation, and a discussion on the maximum work production rate obtainable from it, is done as a first step to a further analysis of the physical limit to its concentration and as a necessary introduction to understand the concept of etendue.

In chapter two etendue and its conservation from the point of view of thermodynamics are introduced. Both issues can be seen as central in this field and are the pillars on which the rest of the thesis stands. The chapter concludes defining the thermodynamic concentration limit of solar radiation which will be used, *a posteriori*, as a reference to

understand state of the art concentrators' potential for improvement always from the point of view of the concentration.

Chapter three starts with a review of the parabolic trough collector's optics. A symmetric non imaging Parametric Trough Collector (PmTC) is proposed. The new concentrator is designed guaranteeing etendue matching for a flat absorber. The flat absorber can be replaced with a multi-tube receiver supported by a thermal insulating base and with transparent covers similar – in section – to the receiver used in the Compact Linear Fresnel Concentrator (CLFC) developed in Australia by Mills (Mills D.R., 2000) for Direct Steam Generation (DSG). The optical design method and the design assumptions are explained. A numerical shape optimization is run and an analysis of the characteristics of the final optics and its merits through comparisons with state of the art optics is performed. The proposed concentrator adds geometrical flexibility that may help to reduce the wind loads and may also allow the definition of a less expensive structure with a better controlled separation between the primary reflector and the ensemble absorber - secondary.

In chapter four a new symmetric non imaging Parametric Trough Collector (PmTC) for a circular evacuated receiver in this case is proposed, applicable for oil or molten salts as heat transfer fluid but also for DSG. In this case the secondary concentrator can be manufactured by partially mirroring a diameter adapted glass tube - either internally or externally - or alternatively by means of a commercial evacuated receiver and an independent arc of circumference external secondary reflector. The optical design method and the design assumptions are explained. A sensitivity study is run and an analysis of the characteristics of the final optics and its merits through comparisons with state of the art optics is performed. The proposed concentrator adds also geometrical flexibility regarding wind loads and maintains high rim angles and a controlled separation between the primary reflector and the ensemble absorber - secondary.

As Fresnel concentrators and Parabolic or Parametric Trough concentrators share the same concentration limit, a comparison in terms of concentration ratio relative to the maximum thermodynamic limit among all of current state of the art Fresnel solutions is done in chapter five. It is out of the scope of this thesis to compare Fresnel concentrators with Parabolic or Parametric Trough concentrators at a plant level. In depth studies analyzing in detail total optical losses (including cosine losses), receiver geometry with thermal losses, plant configuration and costs should be necessary to address the mentioned comparison at plant level.

In chapter six, Computational Fluid Dynamics (CFD) has been used as a “virtual” wind tunnel to compare the flow around a single module of the two PmTCs. Velocity vector field and mean values of aerodynamic coefficients were computed in a range of pitch angles and compared with commercial PTCs (LS2 y LS3 / Eurotrough). Two case studies - 2D and 3D simulations - have been analyzed. Results confirm that the PmTC for circular receiver behaves very similarly to the LS2 and LS3 geometries for the drag, lift and moment coefficients. The PmTC for flat absorber shows the worst performance in comparison with the other three collectors. In addition all rays suffer two reflections before reaching the absorber in this collector while 15% of the rays undergo secondary reflection before arriving to the absorber in the case of the PmTC for circular receiver. These facts and the non-availability of a commercial solution for such kind of receiver have induced the author to select the solution for circular receiver with commercial evacuated receiver an external secondary as the option to be evaluated at plant level in comparison with current PTC technology.

In chapter seven a commercial 50 MWe oil PTC power plant model without thermal energy storage located in Seville (Spain) is build up. A second simulation is run with the proposed PmTC. The collector area was chosen similar to the area of the PTC to assure similar single loop mass flow rates. Since the anidolic designs ignore transmission, absorption and reflection optical losses; calculations of the optical efficiency by means of Montecarlo raytracing simulations using real slope errors distributions and considering Fresnel losses were performed. Annual simulations allowing thermal losses and electricity annual electricity yield calculations allow the final comparison to be made.

OBJECTIVES

There exist two well differentiated R&D strategies undertaken to improve the cost of electricity of current parabolic trough solar thermal plant systems. The first one deals with the development of larger parabolic through collectors which implies a higher demand in tracking accuracy and lower tolerances with respect to wind loads, quality of mirrors, control and mounting imprecision. With this strategy, even if the concentration is improved, the ratio concentration relative to the thermodynamic maximum limit remains constant for the same rim angle. The second strategy develops non imaging concentrators with the aim of bringing the concentration ratio relative to the maximum as close to one as possible or, similarly, improving the geometric concentration without penalising investments in improving accuracy and tolerances.

In that regard, the main objective of this thesis has been the use of Non-imaging Optics to look for new geometries that can improve current commercial parabolic collector's optical, thermal and structural efficiencies respectively to increase the operation temperature and improve global efficiency.

From a structural point of view, optical designs allowing wind load reduction strategies like gaps in the mirrors or large rim angles to control the separation between the absorber and the reflector can contribute toward a more competitive technology both in terms of cost and performance. Therefore structure is highly linked to optics so the use of non-imaging optics can add additional flexibility toward accomplishing the goals mentioned above.

With all this and based on self-experience and in a profound literature review not only in parabolic trough collectors but also in Fresnel collectors the following specific targets are stated:

- i) Obtain a significant optical improvement compared to the Eurotrough / LS3 collector bringing the concentration ratio relative to the maximum as close to one as possible and minimizing the percentage of rays reflected in the secondary reflector before arriving to the absorber.
- ii) Add geometrical flexibility that may help to reduce wind loads while maintaining large rim angles. This may allow the definition of a less expensive structure with a controlled separation between the primary reflector and the

ensemble absorber – secondary and adds value in comparison with the state of the art non-imaging optical solutions.

iii) Evaluate the potential of the proposed solutions projecting them at power plant level.

1. CHAPTER 1: EXERGY OF THE SUN RADIATION

An account of the energy arriving to the earth and its posterior concentration cannot be regarded as complete without a discussion of the sun, the solar system, and the place of the earth within this system (Duffie J.A., 1980).

The sun is a sphere of intensely hot gaseous matter with a diameter of 1.39×10^9 m. As seen from the earth, the sun rotates on its axis about once every four weeks. However, it does not rotate as a solid body; the equator takes about 27 days and the polar regions take about 30 days for each rotation. The temperature in the central interior regions is estimated between 8×10^6 to 40×10^6 K and the density is estimated to be about 100 times that of water. The sun is, in effect, a continuous fusion reactor with its constituent gases as the "containing vessel" retained by gravitational forces. Several fusion reactions have been suggested to supply the energy radiated by the sun. The one considered the most important is a process in which hydrogen combines to form helium. The energy produced in the interior of the solar sphere is transferred out to the surface and then radiated into space. A succession of radiative and convective processes occur with successive emission, absorption, and reradiation. The radiation in the sun's core is in the x-ray and gamma-ray parts of the spectrum, with the wavelengths of the radiation increasing as the temperature drops at larger radial distances (Duffie J.A., 1980).

The sun is on average, 1.5×10^{11} m from the earth. The eccentricity of the earth's orbit is such that the distance between the sun and the earth varies by 1.7% around the average value. The radiation emitted by the sun and its spatial relationship to the earth result in a nearly fixed intensity of solar radiation outside the earth's atmosphere. The total power that is incident on the earth's surface from the sun is 1.73×10^{14} kW and this is equivalent to 1.5×10^{18} kWh annually, which is equivalent to 1.9×10^{14} coal equivalent tons (Duffie J.A., 1980).

To the optical engineer, sun light is simply a very small part of the electromagnetic spectrum, sandwiched between ultraviolet and infrared radiation. The visible portion of the electromagnetic spectrum extends from about 380 to about 780 nanometers. What distinguishes this part of the electromagnetic spectrum from the rest is that radiation in this region is absorbed by the photoreceptors of the human visual system and thereby initiates the process of seeing. The Illuminating Engineering Society of North America (IESNA) defines light as "radian energy that is capable of exciting the retina and producing a visual sensation." (Lighting Research Center, 1990). But in order to understand the nature of sun light, there can be at least three answers to the single question of what light is, depending on the experiment used: (i) light consists of rays

that propagate, e.g., rectilinear in homogeneous media, (ii) light is an electromagnetic wave and (iii) light consists of small portions of energy, or so-called photons. The first property is treated by the geometrical optics where a ray is defined as that trajectory which is always perpendicular to the wave fronts. Concerning the second one, the field of optics treating electromagnetic waves - including light – as carriers of energy, momentum, and angular momentum that propagate in vacuum and deduced mathematically from Maxwell's equations (Webb R.H., 1997) is called wave optics. Geometrical optics can be interpreted as a special case of wave optics for very small wavelengths. Finally the interpretation as photons is unexplainable with wave optics. Only the theory of quantum mechanics and quantum field theory can simultaneously explain light as photons and electromagnetic waves. The field of optics treating this subject is generally called quantum optics (Träger F. (Ed.), 2007).

The first part of this thesis revolves around three issues: first, the solar radiation and the maximum work production rate obtainable from it; second, the concept of etendue and its conservation from the point of view of thermodynamics; and third the optimization of the solar radiation concentration by means of solar collectors that maximize the electricity yield of the solar thermal power plant from a geometric optics point of view. Taking into account that etendue is directly related to radiance it is important to start analyzing the thermodynamics of the solar radiation.

1.1 Fundamental expressions for the energy and entropy of the sun radiation

The sun radiates electromagnetic energy in terms of photons and has an effective blackbody temperature of 5777 K. This effective blackbody temperature is the temperature of a blackbody radiating the same amount of energy as does the sun. Other effective temperatures can be defined, for example, that corresponding to the blackbody temperature giving the same wavelength of maximum radiation as solar radiation (about 6300 K). The extraterrestrial spectral distribution of the solar radiation can be seen in Figure 1-1 Solar Spectrum. After the combined effects of water vapor, dust, and adsorption by various molecules in the air, certain frequencies are strongly absorbed and as a result the spectrum received by the earth's surface is modified. In the figure Air Mass (AM) means the ratio of the relative distance that light must travel through the atmosphere to a given location at any given angle to the sea level path straight through the atmosphere (vertically). Air mass zero refers to the absence of atmospheric attenuation at one astronomical unit from the sun. There is no attenuation effect in the space outside the atmosphere, therefore the air mass is regarded as equal to zero and as equal to one when the sun is directly overhead. However, an air mass value of 1.5 corresponding to a solar zenith angle of 48.2° is considered more

representative of average terrestrial conditions and it is commonly used as a reference condition (Sen Z., 2008).

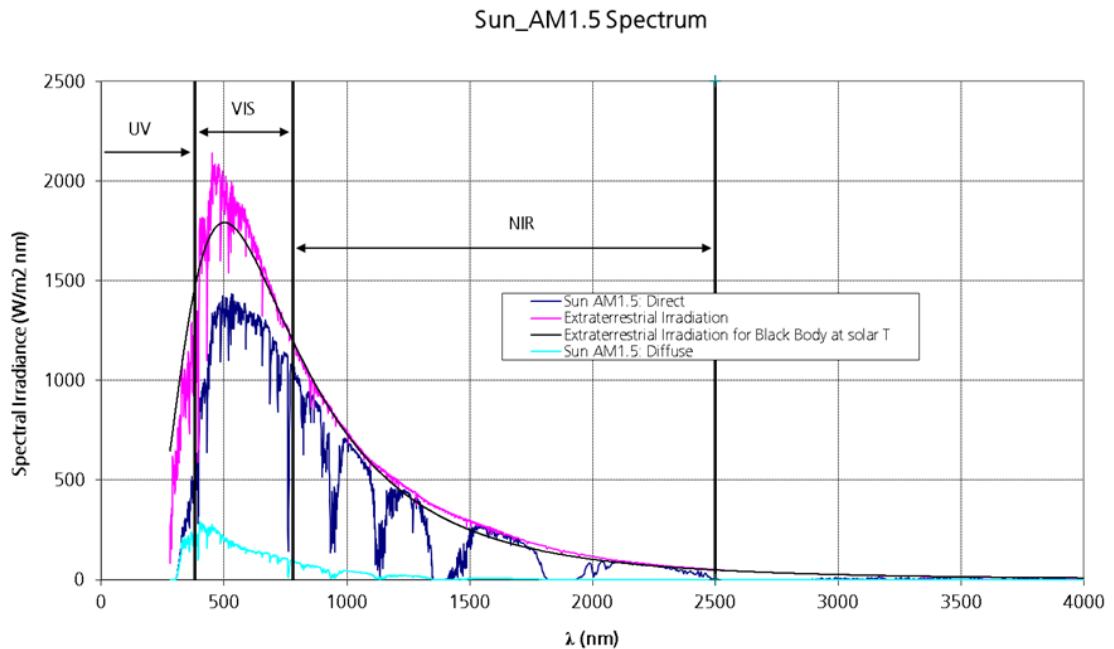


Figure 1-1 Solar Spectrum

1.1.1 Planck's Blackbody Formulas

Before the 20th century scientists could not explain the observed BlackBody (BB) emission spectrum of heat radiation. Objects, regardless their physical or chemical character, were observed to begin glowing "red hot" at the same temperature. The radiation emitted was continuous, rather than in bands or lines, and was determined completely by one parameter, the temperature T.

At the turn of the century, Maxwell introduced the general electromagnetic equations describing the current oscillations in wires. He stated that the frequency of the current oscillations was equal to that of the electromagnetic waves generated, and the electromagnetic waves behaved in every way like light. This lead to the understanding that light was a type of electromagnetic wave created by extremely high frequency electric oscillators in matter. The success of Maxwell's theory motivated scientists to apply it to the long standing puzzle of explaining the Blackbody Radiation (BR) spectrum emitted by a "glowing" solid (Wright S., 1998).

Wien's exponential law was as far as one could get using Maxwell's equations and thermodynamics. This law was loosely based on Maxwell's velocity distribution for gas molecules and agreed very well with experimental results at high frequency. This was because Wien's law actually stated the limiting form

$$K_{\nu,b}(\nu, T) \propto \nu^3 e^{(-B\nu/T)} \quad (1.1)$$

of the blackbody formula for high frequency where B is a constant later found equal to h/k . Planck then stated that the other limiting form of the blackbody formula at low frequencies was:

$$K_{\nu,b}(\nu, T) \propto \nu^2 T \quad (1.2)$$

Planck used mathematical interpolation between the two limiting forms to obtain the **blackbody spectral energy radiance** formula (Planck M., 1914) in $\text{W}/(\text{m}^2 \cdot \text{sr} \cdot \text{Hz})$:

$$K_{\nu,b}(\nu, T) = \frac{ph\nu^3}{c^2} \frac{1}{\left(e^{(h\nu/kT)} - 1\right)} \quad (1.3)$$

where:

$K_{\nu,b}$ = spectral energy radiance of the blackbody in $\text{W}/(\text{m}^2 \cdot \text{sr} \cdot \text{Hz})$

ν = frequency in Hz

T = thermodynamic temperature of the emitting body in K

h = Planck's constant = $6.626 \times 10^{-34} \text{ J}\cdot\text{s}$

c = the speed of light = $2.9979 \times 10^8 \text{ m/s}$

k = Boltzman's constant = $1.38 \times 10^{-23} \text{ J/K}$

p represents the state of polarization of the radiation: $p = 1$ for polarized radiation and $p = 2$ for unpolarized radiation (Landsberg P.T., 1989). The direct radiation is, as is the extraterrestrial radiation, completely unpolarized. Scattering and reflection of the extraterrestrial radiation within the atmosphere result in some degree of polarization of the diffusive part (Kabelac S., 2008).

The **blackbody energy radiance** for unpolarized radiation can be calculated by integration of $K_{\nu,b}$ over frequency in $\text{W}/(\text{m}^2 \cdot \text{sr})$:

$$K_b(T) = \frac{2h}{c^2} \int_0^\infty \frac{\nu^3 d\nu}{\left(e^{(h\nu/kT)} - 1\right)} = \frac{2k^4 T^4}{h^3 c^2} \int_0^\infty \frac{x^3 dx}{\left(e^x - 1\right)} = \frac{15\sigma}{\pi^5} T^4 \int_0^\infty \frac{x^3 dx}{\left(e^x - 1\right)} = \frac{\sigma}{\pi} T^4 \quad (1.4)$$

where:

$$d\nu = \frac{kT}{h} dx \quad (1.5)$$

$$\nu = \frac{kT}{h} x \quad (1.6)$$

$$\sigma = \frac{2\pi^5 k^4}{15h^3 c^2} \quad (1.7)$$

being σ the Stefan-Boltzmann constant.

Planck then proceeded to explain his results from an equilibrium statistical thermodynamics perspective. The thermally agitated resonators have a distribution of vibrational frequencies. To get agreement with experiments Planck postulated that the vibrational energy of each oscillator in a solid was confined to discrete energy levels (quantized):

$$E_{vib} = nh\nu \quad (1.8)$$

where n is a positive integer, h is the Planck's constant, and ν is the vibrational frequency. It was later noticed that the vibrational energy of any system (pendulum, springs, complex systems, etc.) is quantized but for most systems the frequency is such that the smallest quanta of vibrational energy ($h\nu$) is too small to be measured. As a result, Planck arrived at the **blackbody spectral entropy radiance** $L_{v,b}$ formula in $\text{W}/(\text{m}^2 \text{sr}\cdot\text{K}\cdot\text{Hz})$:

$$L_{v,b}(\nu, K_{v,b}) = \frac{pk\nu^2}{c^2} \left[\left(1 + \frac{c^2 K_{v,b}}{ph\nu^3} \right) \ln \left(1 + \frac{c^2 K_{v,b}}{ph\nu^3} \right) - \left(\frac{c^2 K_{v,b}}{ph\nu^3} \right) \ln \left(\frac{c^2 K_{v,b}}{ph\nu^3} \right) \right] \quad (1.9)$$

that can also be expressed in terms of ν and T :

$$L_{v,b}(v, T) = \frac{pk\nu^2}{c^2} \left[\left(1 + \frac{1}{e^{(\hbar\nu/kT)} - 1} \right) \ln \left(1 + \frac{1}{e^{(\hbar\nu/kT)} - 1} \right) - \left(\frac{1}{e^{(\hbar\nu/kT)} - 1} \right) \ln \left(\frac{1}{e^{(\hbar\nu/kT)} - 1} \right) \right] \quad (1.10)$$

The monochromatic entropy flux $L_{v,b}$ is dependent on the energy flux $K_{v,b}$ and the frequency ν only. Monochromatic radiation is the name used for radiation with a single frequency but real radiation is composed of a finite frequency interval. As a result, radiation with an arbitrary spectrum is a superposition of monochromatic rays that do not interact with each other (Wright S., 1998).

Integrating in the whole emission spectrum for unpolarized radiation it can be obtained the extraterrestrial **blackbody entropy radiance**¹ in $\text{W}/(\text{m}^2 \cdot \text{K} \cdot \text{sr})$:

$$\begin{aligned} L_b(T) &= \frac{2k^4 T^3}{h^3 c^2} \int_0^\infty \left[\left(1 + \frac{1}{e^x - 1} \right) \ln \left(1 + \frac{1}{e^x - 1} \right) - \left(\frac{1}{e^x - 1} \right) \ln \left(\frac{1}{e^x - 1} \right) \right] x^2 dx = \\ &= \frac{15\sigma}{\pi^5} T^3 \int_0^\infty \left[\left(1 + \frac{1}{e^x - 1} \right) \ln \left(1 + \frac{1}{e^x - 1} \right) - \left(\frac{1}{e^x - 1} \right) \ln \left(\frac{1}{e^x - 1} \right) \right] x^2 dx = \\ &= \frac{15\sigma}{\pi^5} \frac{4\pi^4}{45} T^3 = \frac{4\sigma}{3\pi} T^3 = \frac{4}{3} \frac{K_b(T)}{T} \end{aligned} \quad (1.11)$$

1.1.2 The sun as a blackbody radiator.

Due to its nature, mathematical treatment of sun radiation and radiation in general involves the extensive use of the spherical coordinate system (Incropera F.P., 2007). From Figure 1-2 The solid angle subtended by dA_n at a point on dA_1 (Incropera F.P.,

¹ Based on:

$$\begin{aligned} &\int_0^\infty \left[\left(1 + \frac{1}{e^x - 1} \right) \ln \left(1 + \frac{1}{e^x - 1} \right) - \left(\frac{1}{e^x - 1} \right) \ln \left(\frac{1}{e^x - 1} \right) \right] x^2 dx = \\ &= \int_0^\infty \left[\ln \left(1 + \frac{1}{e^x - 1} \right) + \left(\frac{1}{e^x - 1} \right) \ln \left(\frac{1 + \frac{1}{e^x - 1}}{\frac{1}{e^x - 1}} \right) \right] x^2 dx = \\ &= \int_0^\infty \left[\ln \left(\frac{1}{1 - e^{-x}} \right) + \left(\frac{1}{e^x - 1} \right) \ln e^x \right] x^2 dx = \int_0^\infty x^2 \ln \left(\frac{1}{1 - e^{-x}} \right) dx + \int_0^\infty \frac{x^3}{e^x - 1} dx = \frac{\pi^4}{45} + \frac{\pi^4}{15} = \frac{4\pi^4}{45} \end{aligned}$$

2007), the differential solid angle $d\Omega$ is measured as the ratio of the area dA_n on the sphere to the square of sphere's radius:

$$d\Omega \equiv \frac{dA_n}{r^2} \quad (1.12)$$

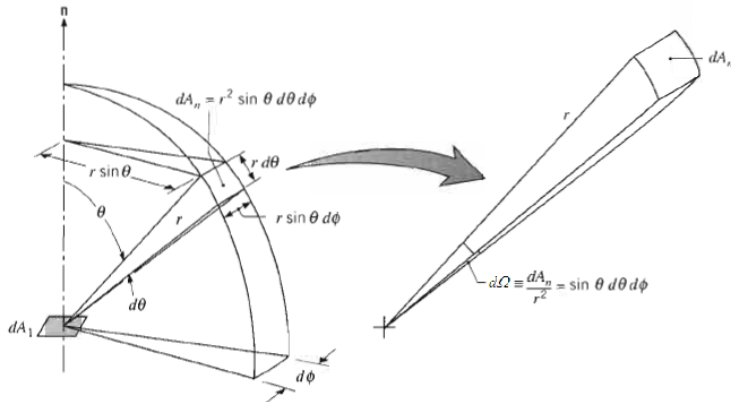


Figure 1-2 The solid angle subtended by dA_n at a point on dA_1 (Incropera F.P., 2007)

Considering the emission in a particular direction from an element of surface area dA_1 as shown in Figure 1-2 The solid angle subtended by dA_n at a point on dA_1 (Incropera F.P., 2007) **Error! Reference source not found.**the direction may be specified in terms of the zenith and azimuthal angles, θ and ϕ , respectively, of a spherical coordinate system. The area dA_n , through which the radiation passes, subtends a differential solid angle $d\Omega$ when viewed from a point on dA_1 . As shown in Figure 1-2 The solid angle subtended by dA_n at a point on dA_1 (Incropera F.P., 2007), the area dA_n is a rectangle of dimension $r d\theta \times r \sin \theta d\phi$; thus:

$$dA_n = r^2 \sin \theta d\theta d\phi \quad (1.13)$$

We now consider the rate at which emission from dA_1 passes through dA_n . From Figure 1-3 The projection of dA_1 normal to the direction of radiation (Incropera F.P., 2007), it can be seen that this projected area is equal to $dA_1 \cos \theta$. In effect it is how dA_1 would appear to an observer situated on dA_n .

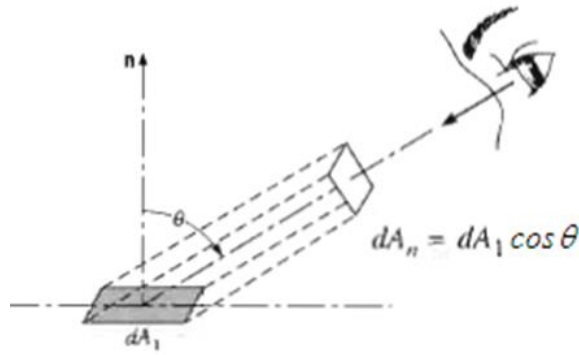


Figure 1-3 The projection of dA_1 normal to the direction of radiation (Incropera F.P., 2007)

If area dA_1 emits (or is crossed) by radiation of a flux $d\Phi_b$ (power) at an angle θ to its normal and this flux is contained inside a solid angle $d\Omega$, the **energy radiance** can be obtained in $\text{W}/(\text{m}^2 \cdot \text{sr})$ as:

$$K_b(T) = \frac{d\Phi_b}{dA_1 \cos \theta d\Omega} \quad (1.14)$$

Integrating in the hemisphere above dA_1 (see Figure 1-4 Emission from a differential element of area dA_1 into a hemisphere centered on dA_1 (Incropera F.P., 2007)) and making $p=2$ it can be found the **energy irradiance** emitted in W/m^2 :

$$\begin{aligned} \Phi_b(T) &= K_b(T) \int_0^{2\pi} \int_0^{\pi/2} \cos \theta \sin \theta d\theta d\phi = \\ &= K_b(T) 2\pi \left[\frac{1}{2} \sin^2 \theta \right]_0^{\pi/2} = \pi \cdot K_b(T) \end{aligned} \quad (1.15)$$

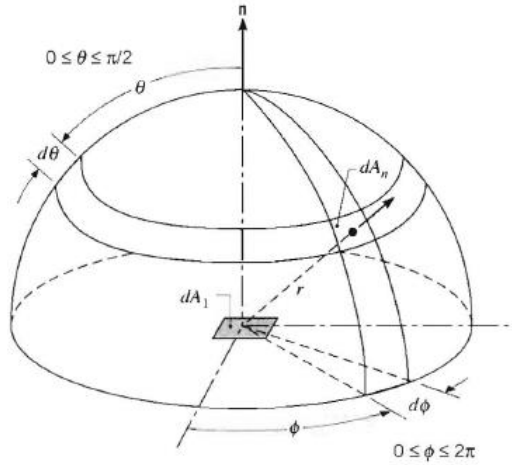


Figure 1-4 Emission from a differential element of area dA_1 into a hemisphere centered on dA_1
(Incropera F.P., 2007)

Note that Φ_b is a flux based on the actual surface area, whereas radiance K_b is based on the projected area. The $\cos \theta$ term appearing in the integrand is a consequence of this difference.

The **rate of photons emitted per unit area, N** , in photons/(m² s) is:

$$N(T) = \frac{\pi \cdot K_b(T)}{E} = \frac{2\pi}{c^2 h^3} \int_0^\infty \frac{E^2 dE}{\left(e^{E/kT} - 1\right)} \quad (1.16)$$

Integrating the energy radiance in the whole sphere ² (see Figure 1-5 Particle emitting in the sphere) and dividing by the energy of one photon the **intensity of the radiation field, I** , in photons/(m² · sr · Hz) can be calculated. The intensity of the radiation field is the number of photons emitted by a blackbody in the whole sphere per unit bandwidth, per unit area and, per unit time. In the case of air (refractive index n=1) we have:

²

$$\int_0^{2\pi} \int_0^{\pi} \sin \theta d\theta d\phi = 4\pi$$

$$\cos \theta = 1$$

$$I(\nu, T) = \frac{K_{\nu,b}(\nu, T) \cdot \int_0^{2\pi} \int_0^{\pi} \sin \theta d\theta d\phi}{h\nu} = \frac{K_{\nu,b}(\nu, T) \cdot 4\pi}{h\nu} = \frac{8\pi\nu^2}{c^2} \frac{1}{\left(e^{\frac{(h\nu)/kT}{c}} - 1\right)} \quad (1.17)$$

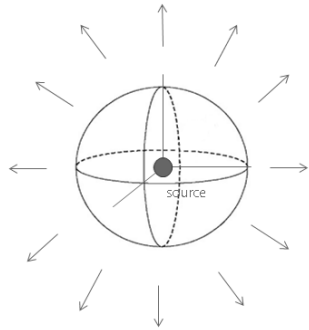


Figure 1-5 Particle emitting in the sphere

In addition, the **energy emitted per unit volume**, U , can be obtained in J/m³ as:

$$U(T) = K_b(T) \frac{\int_0^{2\pi} \int_0^{\pi} \sin \theta d\theta d\phi}{c} = \frac{4\pi}{c} \cdot K_b(T) \quad (1.18)$$

And the **rate of photons emitted per unit volume**, n , in photons/m³, results in:

$$n(T) = \frac{4\pi \cdot K_b(T)}{c \cdot E} = \frac{8\pi}{c^3 h^3} \int_0^\infty \frac{E^2 dE}{\left(e^{\frac{E}{kT}} - 1\right)} \quad (1.19)$$

Similarly the **entropy rate (per unit time) irradiance**, Ψ_b , emitted in the hemisphere can be calculated as W/(m² K):

$$\Psi_b(T) = L_b(T) \int_0^{2\pi} \int_0^{\pi/2} \cos \theta \sin \theta d\theta d\phi = \pi L_b(T) \quad (1.20)$$

And the **entropy emitted per unit volume**, S , in the whole sphere in J/(m³ K):

$$S(T) = L_b(T) \frac{\int_0^{2\pi} \int_0^{\pi} \sin \theta d\theta d\phi}{c} = \frac{4\pi}{c} \cdot L_b(T) \quad (1.21)$$

Particularizing the energy and the entropy emitted per unit volume for blackbody radiation in the whole emission spectra using equations 1.4 and 1.11 one can obtain:

$$U_b(T) = \frac{4\sigma}{c} T^4 = \frac{8\pi^5 k^4}{15h^3 c^3} T^4 = a T^4 \quad (1.22)$$

and:

$$S_b(T) = \frac{4}{3} a T^3 \quad (1.23)$$

being:

$$a = \frac{8\pi^5 k^4}{15h^3 c^3} \quad (1.24)$$

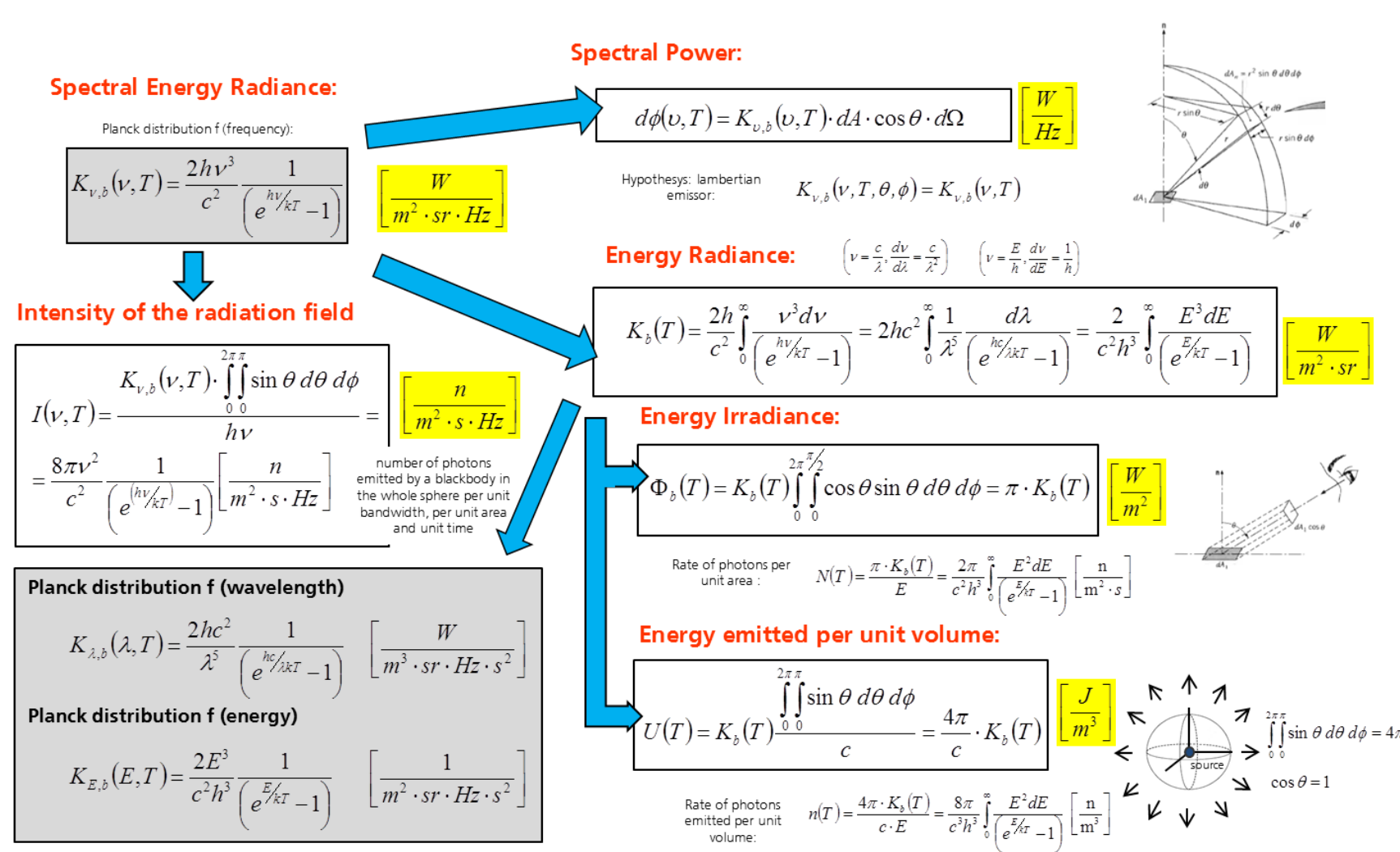


Figure 1-6 Black body (unpolarized) radiation – Power scheme

Spectral Entropy Radiance:

Planck distribution f (frequency):

$$L_{v,b}(v, T) = \frac{2k\nu^2}{c^2} \left[\left(1 + \frac{1}{e^{(\hbar\nu/kT)} - 1} \right) \ln \left(1 + \frac{1}{e^{(\hbar\nu/kT)} - 1} \right) - \left(\frac{1}{e^{(\hbar\nu/kT)} - 1} \right) \ln \left(\frac{1}{e^{(\hbar\nu/kT)} - 1} \right) \right] \left[\frac{W}{m^2 \cdot K \cdot sr \cdot Hz} \right]$$

Entropy Radiance:

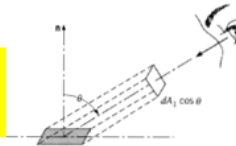
$$L_b(T) = \int_0^\infty L_{v,b}(T) d\nu$$

$$\left(\nu = \frac{c}{\lambda}, \frac{d\nu}{d\lambda} = \frac{c}{\lambda^2} \right) \quad \left(\nu = \frac{E}{h}, \frac{d\nu}{dE} = \frac{1}{h} \right)$$

$$\left[\frac{W}{m^2 \cdot K \cdot sr} \right]$$

Entropy Irradiance:

$$\Psi_b(T) = L_b(T) \int_0^{2\pi} \int_0^{\pi/2} \cos \theta \sin \theta d\theta d\phi = \pi \cdot L_b(T) \left[\frac{W}{m^2 \cdot K} \right]$$



Entropy emitted per unit volume:

$$S(T) = L_b(T) \frac{\int_0^{2\pi} \int_0^{\pi} \sin \theta d\theta d\phi}{c} = \frac{4\pi}{c} \cdot L_b(T) \left[\frac{J}{m^3 \cdot K} \right]$$

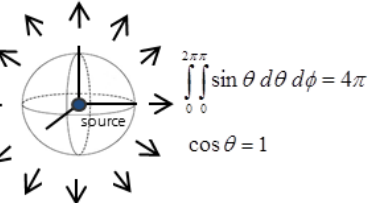


Figure 1-7 Black body (unpolarized) radiation – Entropy scheme

1.2 Maximum possible useful work from sun radiation

As the sun emits isotropically in all directions, when light reaches the earth is confined to a cone of angle 2δ as shown in Figure 1-8. Light emitted by the sun that reaches the earth is confined within a cone of angle 2δ . Imaging the sun as a spherically symmetric source of radiant energy it is possible to give a thermodynamic argument in the context of solar energy concentration. The flux falls off as the inverse square of the distance d from the center, as follows from the conservation of power through successive spheres of area $4\pi d^2$. Therefore, the flux on the earth's surface (A_1 in figure), is smaller than the solar surface flux by a factor $(r/d)^2$, where r is the radius of the sun and d is the distance from the earth to the sun. By simple geometry, $r/d = \sin\delta$ where δ is the angular subtense (half angle) of the sun. Accepting the premise that no terrestrial device can boost the flux above its solar surface value (which would lead to a variety of perpetual motion machines), then the limit to concentration is just $(1/\sin\delta)^2$. This limit is called the sine law of concentration (Winston R., 2005).

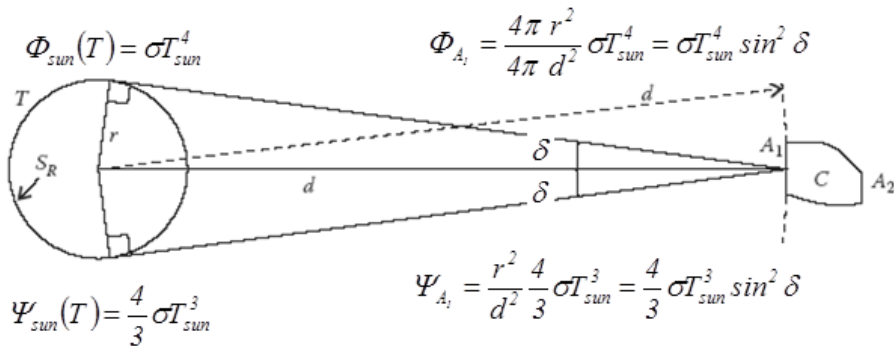


Figure 1-8 Light emitted by the sun that reaches the earth confined within a cone of angle 2δ . Entropy rate and the power irradiance balance.

Considering the values depicted in section 1 for the sun geometry and its distance to the earth one can obtain:

- the angular subtense of the sun

$$\delta = a \tan\left(\frac{r}{d}\right) = 4.65 \text{ mrad} \quad (1.25)$$

- the earth intercepts 0.00216% of the total power emitted by the sun:

$$\sin^2 \delta = 2.16 \cdot 10^{-5} \quad (1.26)$$

- the solid angle subtended by sun from earth:

$$\Omega_s = \int_0^{2\pi} \int_0^\delta \sin \theta d\theta d\phi = 2\pi(1 - \cos \delta) = 6.79 \cdot 10^{-5} \text{ sr} \quad (1.27)$$

Additionally, the power irradiance arriving to the earth and the entropy rate can be calculated as:

$$\begin{aligned} \Psi_{A1}(T) &= L_b(T) \int_0^{2\pi} \int_0^\delta \cos \theta \sin \theta d\theta d\phi = L_b(T) 2\pi \left[\frac{1}{2} \sin^2 \theta \right]_0^\delta = \\ &= \frac{4\sigma}{3\pi} 2\pi T_{sun}^3 \left(\frac{1}{2} \sin^2 \delta \right) = \frac{4}{3} \sigma T_{sun}^3 \sin^2 \delta \end{aligned} \quad (1.28)$$

$$\begin{aligned} \Phi_{A1}(T) &= K_b(T) \int_0^{2\pi} \int_0^\delta \cos \theta \sin \theta d\theta d\phi = K_b(T) 2\pi \left[\frac{1}{2} \sin^2 \theta \right]_0^\delta = \\ &= \frac{\sigma T_{sun}^4}{\pi} 2\pi \left(\frac{1}{2} \sin^2 \delta \right) = \sigma T_{sun}^4 \sin^2 \delta \end{aligned} \quad (1.29)$$

If exergy is defined as the maximum possible useful work obtainable from a reversible process on a system at temperature T in the presence of an infinite environment of temperature T_0 (Landsberg P. T, 1979), the exergy of the sun radiation arriving to the earth can be calculated in W/m^2 as:

$$\begin{aligned} Ex_{A1} &= \Phi_{A1} - T_0 \Psi_{A1} = \left[\sigma (T_{sun}^4 - T_0^4) - \frac{4}{3} \sigma T_0 (T_{sun}^3 - T_0^3) \right] \sin^2 \delta = \\ &= \sigma \sin^2 \delta \left(T_{sun}^4 - T_0^4 - \frac{4}{3} T_0 T_{sun}^3 + \frac{4}{3} T_0^4 \right) = \sigma \sin^2 \delta \left(T_{sun}^4 - \frac{4}{3} T_0 T_{sun}^3 + \frac{1}{3} T_0^4 \right) = \\ &= \sigma T_{sun}^4 \sin^2 \delta \left(1 - \frac{4}{3} \frac{T_0}{T_{sun}} + \frac{1}{3} \frac{T_0^4}{T_{sun}^4} \right) \end{aligned} \quad (1.30)$$

being T_0 the ambient temperature and T_{sun} the sun effective blackbody temperature. Calculating for typical ambient temperatures and for $T_{sun} = 5777 \text{ K}$ the exergetic efficiency can be obtained as:

$$\eta Ex_b = \eta_L = 1 - \frac{4}{3} \frac{T_0}{T_{sun}} + \frac{1}{3} \frac{T_0^4}{T_{sun}^4} = 0.93 \quad (1.31)$$

which is an upper limit to the conversion efficiency of the sun energy known as the Landsberg efficiency.

We can arrive to the same result with a different approach. If we analyze the space of volume V delineated by a diffuse reflector surface that reflects 100% of the incident radiation in Figure 1-9 Enclosure with perfectly reflecting internal surfaces (Bejan A., 2006) where we introduce a blackbody B that absorbs entirely the incident radiation regardless of frequency, the isolated V volume will be filled by photons of all frequencies and, in equilibrium, the temperature T_B that is reached by the blackbody can also be assigned to the radiation with which the blackbody is in equilibrium (Bejan A., 2006).

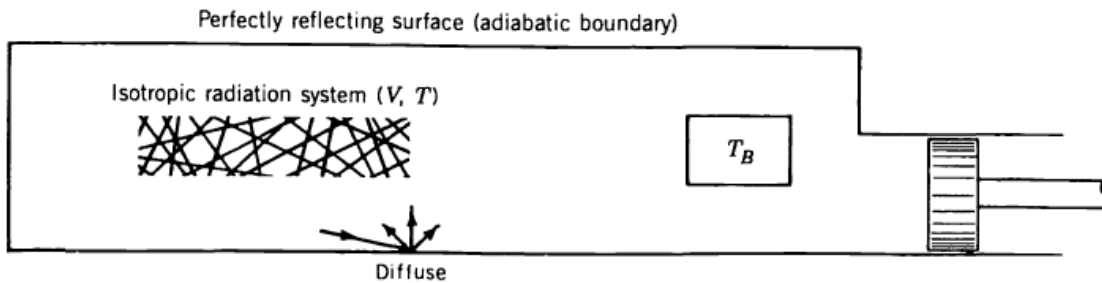


Figure 1-9 Enclosure with perfectly reflecting internal surfaces (Bejan A., 2006)

If one of the walls of the perfectly reflecting enclosure could move like a piston inside a frictionless sleeve, the environment must restrain this movement by applying pressure on the piston the pressure exerted by the trapped radiation in form of photon gas can be obtained, using equation 1.24, as (Bejan A., 2006):

$$P_b(T) = \frac{1}{3} U_b(T) = \frac{a}{3} T^4 \quad (1.32)$$

In the case of a reversible and adiabatic expansion or compression the entropy remains constant and:

$$\frac{4}{3} a V T^3 = \text{constant} \rightarrow V T^3 = \text{constant} \quad (1.33)$$

$$V P_b^{3/4} = \text{constant} \quad (1.35)$$

The reversible work transfer between states 1 and 2 is then:

$$\begin{aligned}
 W_{1-2,rev} &= \int_1^2 P_b dV = \text{constant}^{\frac{4}{3}} \int_1^2 V^{-\frac{4}{3}} dV = -3 \cdot \text{constant}^{-\frac{4}{3}} \cdot \left(\frac{1}{V_2^{\frac{1}{3}}} - \frac{1}{V_1^{\frac{1}{3}}} \right) = \\
 &= 3 \frac{\text{constant}^{\frac{4}{3}}}{V_1^{\frac{1}{3}}} \left[1 - \left(\frac{V_1}{V_2} \right)^{\frac{1}{3}} \right] = 3P_1V_1 \left[1 - \left(\frac{V_1}{V_2} \right)^{\frac{1}{3}} \right]
 \end{aligned} \tag{1.36}$$

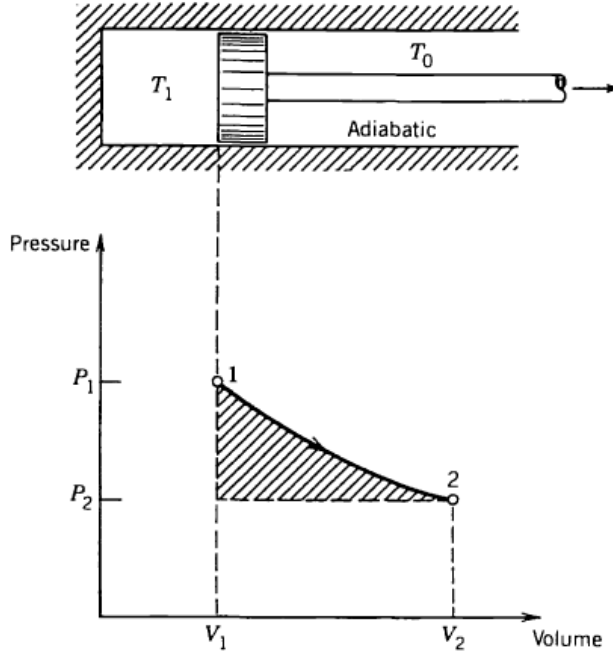


Figure 1-10 Reversible and adiabatic expansion for calculating the non flow exergy of enclosed blackbody radiation (Bejan A., 2006)

If a batch of blackbody radiation (V_1, T_1) is immersed in an environment of blackbody radiation of temperature T_0 for the extraction of maximum work being $T_2=T_0$, Petela proposed the reversible and adiabatic expansion to the end state (V_2, T_2) as shown in Figure 1-10 Reversible and adiabatic expansion for calculating the non flow exergy of enclosed blackbody radiation (Bejan A., 2006). In this case the net work through the piston rod is:

$$\begin{aligned}
 W_{1-2} &= \int_1^2 PdV - P_2(V_2 - V_1) = 3P_1V_1 \left[1 - \left(\frac{V_1}{V_2} \right)^{\frac{1}{3}} \right] - P_2(V_2 - V_1) = 3P_1V_1 \left[1 - \left(\frac{V_1}{V_2} \right)^{\frac{1}{3}} \right] - P_2V_1 \left[\frac{V_2}{V_1} - 1 \right] = \\
 &= U_1V_1 \left[1 - \left(\frac{V_1}{V_2} \right)^{\frac{1}{3}} \right] - \frac{U_1V_1}{3} \left(\frac{T_2}{T_1} \right)^4 \left[\frac{V_2}{V_1} - 1 \right] = U_1V_1 \left[1 - \frac{T_2}{T_1} - \frac{1}{3} \left(\frac{T_2}{T_1} \right)^4 \left[\left(\frac{T_1}{T_2} \right)^3 - 1 \right] \right] =
 \end{aligned}$$

$$= U_1 V_1 \left[1 - \frac{4}{3} \frac{T_2}{T_1} + \frac{1}{3} \left(\frac{T_2}{T_1} \right)^4 \right] \quad (1.37)$$

If we make $T_1=T_{sun}$ and $T_2=T_0$ and analyze the result in terms of efficiency dividing by the original energy inventory of the system, we obtain Petela's limit which coincides with the aforementioned Landsberg's limit:

$$\eta_p = \frac{W_{1-2}}{U_1 V_1} = 1 - \frac{4}{3} \frac{T_0}{T_{sun}} + \frac{1}{3} \frac{T_0^4}{T_{sun}^4} = 0.93 \quad (1.38)$$

2. CHAPTER 2: SOLAR CONCENTRATORS. ETENDUE AND MAXIMUM CONCENTRATION

Geometrical optics is used as the basic tool in designing almost any optical system, image forming or not. This approach uses the intuitive ideas of a ray of light, roughly defined as the path along which light energy travels, together with surfaces that reflect or transmit the light. When light is reflected from a smooth surface, it obeys the well-known law of reflection, which states that the incident and reflected rays form equal angles with the normal to the surface and that both rays and the normal lie in one plane. When light is transmitted, the ray direction is changed according to the law of refraction: Snell's law (Winston R., 2005). This law states that the sine of the angle between the normal and the incident ray bears a constant ratio to the sine of the angle between the normal and the refracted ray; again, all three directions are coplanar (Winston R., 2005).

A major part of the design and analysis of concentrators involves ray tracing, that is, following the paths of rays through a system of reflecting and refracting surfaces. This is a well-known process in conventional lens design, but the requirements are somewhat different for concentrators, so it will be convenient to state and develop the methods *ab initio*. This is because in conventional lens design the reflecting or refracting surfaces involved are mostly always portions of spheres, and the centers of the spheres lie on one straight line (axisymmetric optical system) so that special methods that take advantage of the simplicity of the forms of the surfaces and the corresponding symmetry can be used (Chaves J., 2008).

Imaging optical systems have three main components: the object, the optics, and the image it forms. The object is considered as a set of points that emit light in all directions. The light (or part of it) from each point on the object is captured by the optical system and concentrated onto a point in the image. The distances between points on the image may be scaled relative to those on the object resulting in magnification or reduction.

Non-imaging optical systems, instead of an object, start from a light source and instead of an image finish in a receiver. Instead of an image of the source, the optics produces a prescribed illuminance (or irradiance) pattern on the receiver. The first application of non-imaging optics referred to the design of concentrators that could perform at the maximum theoretical (thermodynamic) limit (Winston R., 2005).

With the foundations established in chapter one now the problem of how to concentrate solar radiation guaranteeing etendue matching in multitubular or circular receivers like the ones used in the state of the art solar plants is here addressed. The objective is generating

geometries with enough flexibility to reduce wind loads while controlling the separation between the primary reflector and the ensemble absorber – secondary.

2.1 The concept of etendue

When light passes through an area dA , it requires “room.” This space has two components: “spatial room” measured by the area and “angular room” measured by the solid angle. Thus, if light crosses this area in a direction θ to its normal, then it “sees” only the projected area $dA \cos \theta$ as the available area for it to pass through.

The etendue is defined as the product of the available spatial room $dA \cos \theta$ and the angular room $d\Omega$ defined by the solid angle. If area dA is in a medium of refractive index n , the expression of the etendue can be rewritten as (Chaves J., 2008):

$$dU = n^2 \cdot dA \cdot \cos \theta \cdot d\Omega = n^2 \cdot dA \cdot \cos \theta \cdot \sin \theta \cdot d\theta \cdot d\varphi \quad (2.1)$$

At stated previously it can be seen that radiation of a flux $d\Phi$ (power) emitted (or crossed) by an area dA_1 forming an angle θ with its normal and contained in a solid angle $d\Omega$ is the energy radiance times the etendue.

$$d\Phi(T) = K(T) dA \cos \theta d\Omega = K(T) dU \quad (2.2)$$

2.1.1 Conservation of etendue

The law of conservation of etendue tells us that etendue remains constant. This means that if the area available for the light is increased, the solid angle decreases. But if the area decreases, the solid angle must increase. For example, to illuminate the interior of a box with the light of three flashlights that emit a beam of light with an angular aperture α and through a large opening AB on the side of the box as in the case of Figure 2-1 Interior of a box illuminated with three flashlights with small angular spread (Chaves J., 2008) the light that the box receives has a small angular aperture α , but is spread out over the area AB. An alternative way of illuminating the interior of the box is to open a smaller hole CD, tilt some of the flashlights, and make the light to pass through this smaller aperture as shown in Figure 2-2 Interior of a box illuminated with three flashlights with large angular spread (Chaves J., 2008). In this case, however, the angular aperture of the light entering the box is larger as indicated by the angle β . To illuminate the interior of the box there are two options: (a) either the area of the hole is large and the angle of the light is small or (b) the area is small, but the angle of the light is large. It is as if the light needed “space” to move through. Either we give it some area (physical space) for it to pass through or, if we diminish the area, we must give it angular space. This example illustrates the law of conservation of etendue.

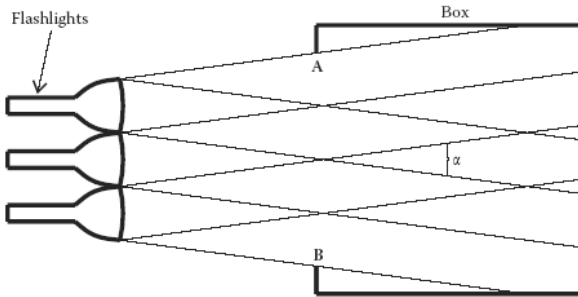


Figure 2-1 Interior of a box illuminated with three flashlights with small angular spread (Chaves J., 2008)

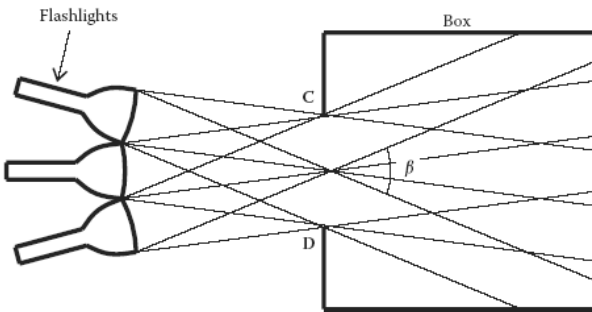


Figure 2-2 Interior of a box illuminated with three flashlights with large angular spread (Chaves J., 2008)

Assume that we have two surfaces dA_1 and dA_2 that are separated by a distance r , the angles that their normals n_1 and n_2 form with the direction r are θ_1 and θ_2 respectively, and the medium between these surfaces has a refractive index $n=1$. If dA_1 emits light toward dA_2 , the etendue of this light is:

$$dU_{12} = n^2 \cdot dA_1 \cdot \cos \theta_1 \cdot d\Omega_{12} = n^2 \cdot dA_1 \cdot \cos \theta_1 \frac{dA_2 \cdot \cos \theta_2}{r^2} = n^2 \cdot \pi \cdot dA_1 \cdot dF_{dA_1-dA_2} \quad (2.3)$$

with $F_{dA_1-dA_2}$ the radiative heat transfer shape factor of an area dA_1 to another area dA_2 .

If dA_2 emits light toward dA_1 , the etendue of this light is:

$$dU_{21} = n^2 \cdot dA_2 \cdot \cos \theta_2 \cdot d\Omega_{21} = n^2 \cdot dA_2 \cdot \cos \theta_2 \frac{dA_1 \cdot \cos \theta_1}{r^2} = n^2 \cdot \pi \cdot dA_2 \cdot dF_{dA_2-dA_1} \quad (2.4)$$

From these two expressions we can conclude that:

$$dU_{12} = dU_{21} \quad (2.5)$$

If the system is in equilibrium the radiation flux $d\Phi_{12}$ that dA_1 emits toward dA_2 equals the radiation flux $d\Phi_{21}$ that dA_2 emits toward dA_1 and thus we have:

$$d\Phi_{12}(T) = d\Phi_{21}(T) \quad (2.6)$$

so:

$$K_1(T) = K_2(T) \quad (2.7)$$

where K_1 is the basic radiance at dA_1 of the light emitted from dA_1 toward dA_2 and K_2 the basic radiance at dA_2 of the light emitted from dA_2 toward dA_1 .

For 2-D systems, the situation is similar. We can now write:

$$\begin{aligned} dU_{12} &= n \cdot da_1 \cdot \cos \theta_1 \cdot d\theta_1 = n \cdot da_1 \cdot \cos \theta_1 \frac{da_2 \cdot \cos \theta_2}{r} = \\ &= 2 \cdot n \cdot da_1 \frac{da_2 \cdot \cos \theta_1 \cdot \cos \theta_2}{2r} = 2 \cdot n \cdot da_1 \cdot F_{da_1-da_2} \end{aligned} \quad (2.8)$$

so the etendue can therefore be related to the shape factor $F_{da_1-da_2}$ of a length da_1 to another length da_2

$$\begin{aligned} dU_{21} &= n \cdot da_2 \cdot \cos \theta_2 \cdot d\theta_2 = n \cdot da_2 \cdot \cos \theta_2 \frac{da_1 \cdot \cos \theta_1}{r} = \\ &= 2 \cdot n \cdot da_2 \frac{da_1 \cdot \cos \theta_2 \cdot \cos \theta_1}{2r} = 2 \cdot n \cdot da_2 \cdot F_{da_2-da_1} \end{aligned} \quad (2.9)$$

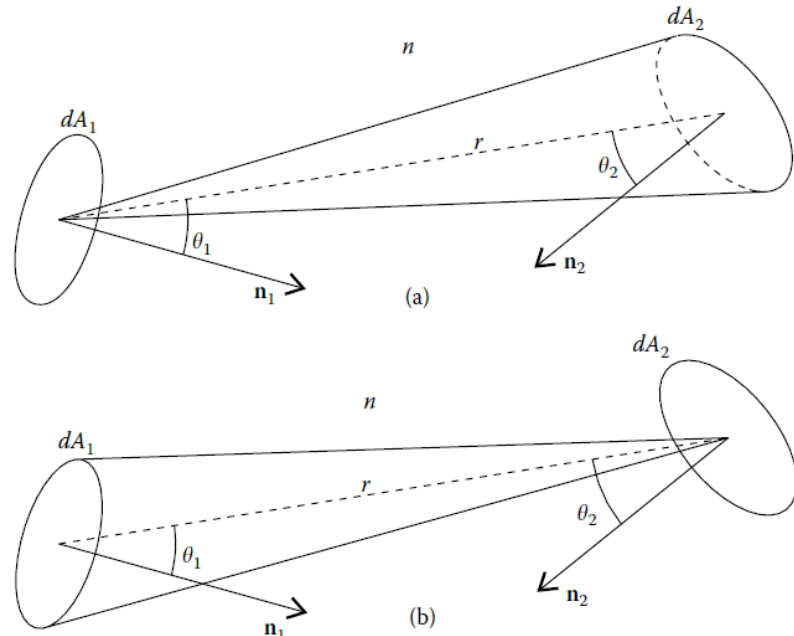


Figure 2-3 3D case: The etendue of the light emitted by dA_1 toward dA_2 equals that of light emitted

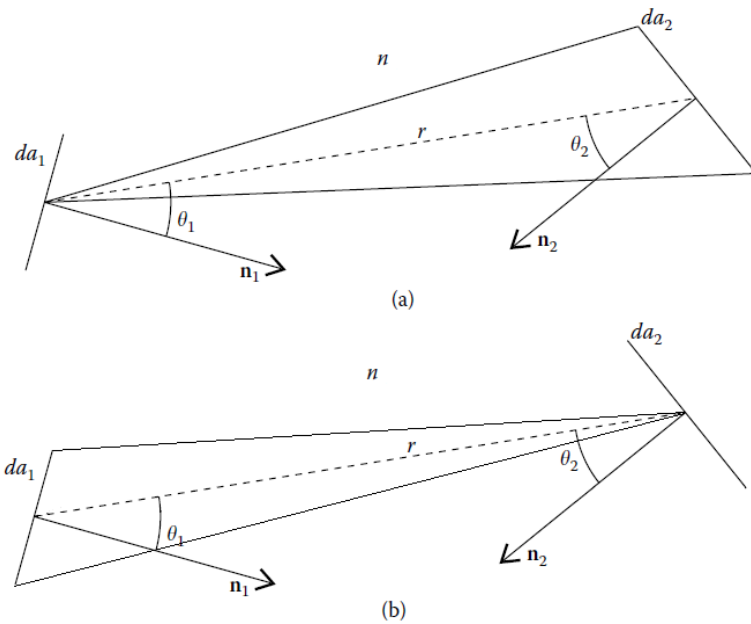


Figure 2-4 2D case: The etendue of the light emitted by da_1 toward da_2 equals that of light emitted

2.1.2 Imperfect optical systems

We have seen that etendue and basic radiance are conserved in optical systems. This, however, is only true in “perfect” optical systems. There exists “imperfect” optics in which etendue may be reduced or increased or in which basic radiance may decrease. In an optical system where the radiance L is conserved (no variations in the refractive index), we may lose etendue if we lose flux. From the expression $\Phi = KU$ (the case in which $n = 1$), if a part of the flux Φ is lost, this means a part of the etendue U is also lost. One possibility for such situation is shown in Figure 3.11, where we have a set of flashlights emitting light with angular aperture α toward a box with a hole EF on its side. When entering the box, part of the light is shaded by the walls and only a part of it passes through the hole. The etendue of the light entering the box is reduced because there is loss of light.

There are also situations in which the basic radiance may decrease. An example is when absorption of light takes place as it travels through a material as shown in Figure 3.12. In this example, we have light with an angular aperture 2α entering a space between two parallel mirrors M_1 and M_2 . At the other side, the area and angular aperture of light are still the same and therefore etendue is also the same. If, on the other hand, the material is absorptive, the light flux decreases and from $\Phi = L \cdot U$ the basic radiance also decreases.

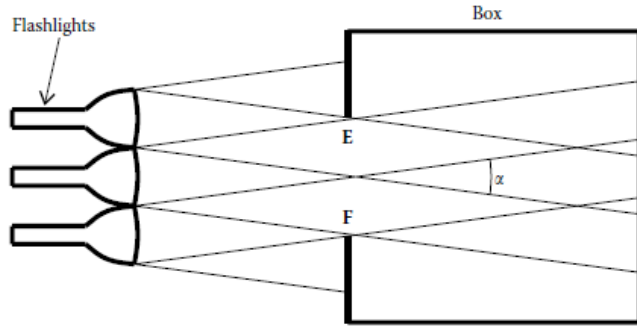


Figure 2-5 Loss of light and etendue in a system that conserves radiance (Chaves J., 2008)

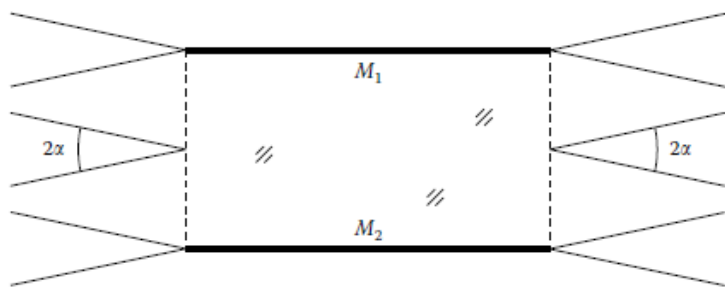


Figure 2-6 Radiance decrease when light travels in an absorptive optical system (Chaves J., 2008)

2.2 Maximum concentration that a solar concentrator can provide

Conservation of etendue can be used to derive the maximum concentration that an optical system can provide. Let us consider a 3D situation and calculate the etendue of radiation with half-angular aperture δ and crossing (or being emitted by) an area A immersed in a medium with a refractive index of $n=1$ as presented in next figure:

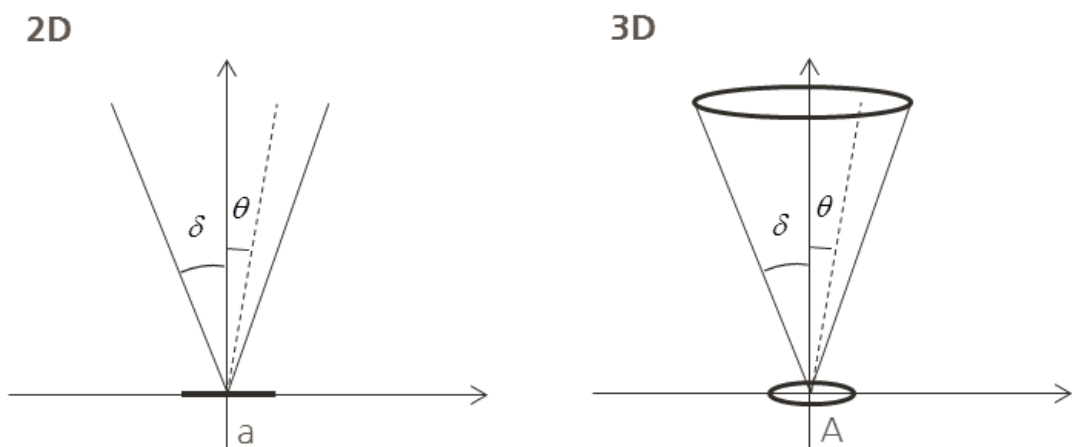


Figure 2-7 Etendue in two and three dimensions (normal incidence)

In the 3D case the etendue of the radiation crossing (or being emitted by) A can be obtained

$$U = n^2 A \int_0^{2\pi} d\varphi \int_0^\delta \cos \theta \cdot \sin \theta \cdot d\theta = \pi \cdot n^2 \cdot A \cdot \sin^2 \delta \quad (2.10)$$

For the 2D case:

$$U = n \cdot a \int_{-\delta}^{\delta} \cos \theta \cdot d\theta = n \cdot 2 \cdot a \cdot \sin \delta \quad (2.11)$$

Applying the 3D result to an optical system with entrance aperture A_1 and exit aperture A_2 , being δ_1 the half-angular aperture for the radiation at the entrance aperture and δ_2 the half-angular aperture at the exit aperture as presented in Figure 2-8 A two dimensional optical device with an entrance aperture a_1 and exit aperture a_2 . At the entrance aperture, the refractive index is n_1 and the half-angular aperture of the radiation is δ_1 . At the exit aperture, the refractive index is n_2 and the half-angular aperture of the radiation is δ_2 (Chaves J., 2008) the etendue at the entrance aperture is:

$$U_1 = \pi \cdot n_1^2 \cdot A_1 \cdot \sin^2 \delta_1 \quad (2.12)$$

If the refractive index at the exit aperture is n_2 , the etendue of the radiation exiting the device is given as:

$$U_2 = \pi \cdot n_2^2 \cdot A_2 \cdot \sin^2 \delta_2 \quad (2.13)$$

Since the etendue at the entrance aperture must be equal to the one at the exit $U_1=U_2$:

$$\frac{A_1}{A_2} = \frac{n_2^2 \cdot \sin^2 \delta_2}{n_1^2 \cdot \sin^2 \delta_1} \quad (2.14)$$

the angle δ_2 at the exit aperture cannot be higher than $\pi/2$; therefore, the minimum exit area $A_{2\min}$ can be obtained for $\delta_2 = \pi/2$. This area corresponds to the maximum possible concentration:

$$C_{\max} = \frac{A_1}{A_{2\min}} = \frac{n_2^2}{n_1^2} \frac{1}{\sin^2 \delta_1} \quad (2.15)$$

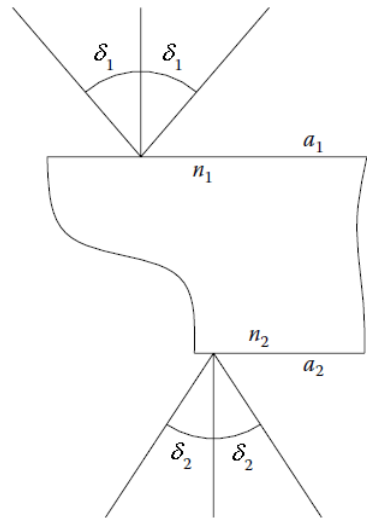


Figure 2-8 A two dimensional optical device with an entrance aperture a_1 and exit aperture a_2 . At the entrance aperture, the refractive index is n_1 and the half-angular aperture of the radiation is δ_1 . At the exit aperture, the refractive index is n_2 and the half-angular aperture of the radiation is δ_2 (Chaves J., 2008)

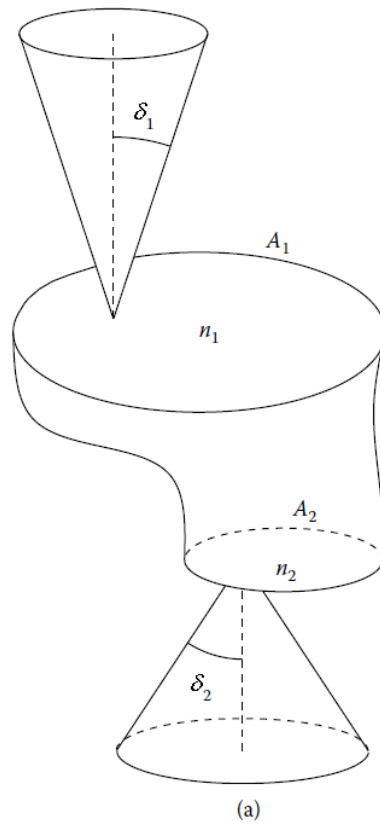


Figure 2-9 A three dimensional optical device with an entrance aperture A_1 and exit aperture A_2 . At the entrance aperture, the refractive index is n_1 and the half-angular aperture of the radiation is δ_1 . At the exit aperture, the refractive index is n_2 and the half-angular aperture of the radiation is δ_2 (Chaves J., 2008)

Let us consider a 2-D optical device with entrance aperture a_1 and exit aperture a_2 . The refractive index at the entrance aperture is n_1 and the half-angular aperture of the radiation is θ_1 . The refractive index at the exit aperture is n_2 and the half-angular aperture of the radiation is θ_2 .

For this 2D optical system with entrance aperture a_1 and exit aperture a_2 we can write:

$$U_1 = n_1 \cdot 2 \cdot a_1 \cdot \sin \delta_1 \quad (2.16)$$

$$U_2 = n_2 \cdot 2 \cdot a_2 \cdot \sin \delta_2 \quad (2.17)$$

$$\frac{a_1}{a_2} = \frac{n_2 \cdot \sin \delta_2}{n_1 \cdot \sin \delta_1} \quad (2.18)$$

$$C_{\max} = \frac{a_1}{a_{2\min}} = \frac{n_2}{n_1} \frac{1}{\sin \delta_1} \quad (2.19)$$

3. CHAPTER 3: OPTICAL ANALYSIS OF A TWO STAGE XX SIMULTANEOUS MULTIPLE SURFACE (SMS) CONCENTRATOR FOR PARAMETRIC TROUGH PRIMARY AND FLAT ABSORBER WITH APPLICATION IN DIRECT STEAM GENERATION (DSG) SOLAR THERMAL PLANTS

This chapter will be published as a paper with the following authors, abstract and keywords:

Authors: **Juan Pablo Núñez Bootello**, email address: jp.nunez@abengoa.com
Abengoa. Calle Energía Solar, 1. Seville 41014, Spain

Henry Price, email address: hank.price@abengoa.com
Abengoa. 1250 Simms Street. Lakewood 80401, USA

Manuel Silva Pérez, email address: msilva@us.es
University of Seville. Group of Thermodynamics and Renewable Energy,
Department of Energy Engineering. Camino de Los Descubrimientos, s/n.
41092- Seville, Spain

Manuel Doblaré Castellano, email address: manuel.doblare@abengoa.com
Abengoa. Calle Energía Solar, 1, Seville 41014, Spain.

Abstract:

Today most commercial Parabolic Trough Collector (PTC) solar power plants make use of the well-known LS3 / Eurotrough optics. The PTC has a concentration ratio relative to the maximum thermodynamic limit equal to 0.31. In order to improve the competitiveness of PTC technology, two well differentiated R&D strategies have been undertaken: i) developing larger parabolic troughs, which places a higher demand in tracking accuracy and lower tolerances with respect to wind loads, quality of mirrors, control and assembly imprecisions, and ii) developing secondary concentrators with the aim of bringing the concentration ratio relative to the maximum one as close to 1 as possible. In this paper, a Parametric Trough Collector (PmTC) for a flat receiver designed with the Simultaneous Multiple Surface (SMS) method is proposed. The method assumes zero transmission, absorption and reflection optical losses and allows for both reflective primary and secondary surfaces (XX - reflective plus reflective) to be simultaneously designed, guaranteeing Etendue matching. The proposed PmTC geometry increases the referred ratio up to 0.59 with a rim angle greater than 100° and with the same effective acceptance angle as the PTC. The flat absorber can be replaced with a multi-tube receiver for application in Direct Steam Generation (DSG).

Keywords: Parabolic trough; Wind loads, SMS method; Non-imaging optics; Concentrated Solar Power, Solar Thermal Electric

References

- Benítez P., García R., Miñano J.C. 1997. Contactless efficient two-stage solar concentrator for tubular absorber. *Appl Opt.* Oct 1;36(28):7119-24
- Benítez P., Miñano J.C., Zamora P., Mohedano R., Cvetkovic A., Buljan M., Chaves J., Hernández M. 2010. High performance Fresnel-based photovoltaic concentrator. *Optics Express*, Vol. 18, Issue S1, pp. A25-A40
- Cannavaro D., Chaves J., Collares M. 2013. New second-stage concentrators (XX SMS) for parabolic primaries; Comparison with conventional parabolic trough concentrators. *Solar Energy*. Volume 92, June, Pages 98–105
- Chaves J. 2008. Introduction to non imaging optics, CRC Press.
- Davies P. A. 1994. The edge ray principle of nonimaging optics. *JOSA A*, Vol. 11, Issue 4, pp. 1256-1259.
- Estela, 2012. Solar Thermal Electricity – Strategic Research Agenda 2020 – 2025, : European Solar Thermal. Electricity Association.
- Fernández-García, Zarza E., Valenzuela L., Pérez M. 2010. Parabolic-trough solar collectors and their applications. *Renewable and Sustainable Energy Reviews*. Volume 14, Issue 7, September, Pages 1695–1721
- Giannuzzi G. M., Majorana C. E., Miliozzi A., Salomoni V. A., Nicolini D. 2007. Structural Design Criteria for Steel Components of Parabolic-Trough Solar Concentrators. *J. Sol. Energy Eng.* 129(4):382-390.
- Lüpfer E., Geyer M., Schiel W., Esteban A., Osuna R., Zarza E., Nava P. 2001. Eurotrough design issues and prototype testing at PSA. *Proceedings of Solar Forum 2001 Solar Energy: The Power to Choose April 21-25*, Washington, DC
- Marcotte P., Manning K. 2013. Development of an advanced large-aperture parabolic trough collector. *Energy Procedia Volume 49*, 2014, Pages 145–154. *Proceedings of the SolarPACES 2013 International Conference*
- Martinez-Val J., Abánades A., Abbas R., Muñoz J., Valdés M., Ramos A., Rovira A., Montes MJ., 2011. Thermal performance analysis of linear receivers. Pages 489–498. *Proceedings of the SolarPACES 2011 International Conference*
- Minano J.C., Gonzalez J.C. 1992. New method of design of nonimaging concentrators. *Applied Optics*, Vol. 31, Issue 16, pp. 3051-3060.
- Pereira M.C., Gordon J.M., Rabl A., Winston R. 1991. High concentration two stage optics for Parabolic Trough Solar Collectors with tubular absorber and large rim angle. *Solar Energy*. Volume 47, Issue 6, Pages 457–466
- Price H., Lüpfer E., Kearney D., Zarza E., Cohen G., Gee R., Mahoney R. 2002. Advances in Parabolic Trough Solar Power Technology. *J. Sol. Energy Eng.* 124(2), 109-125
- Rabl A. 1985. Active Solar Collectors and Their Applications - Oxford U. Press, Oxford, UK.
- Rabl A. 1977. Radiation transfer trough specular passages – a simple approximation. *International Journal of Heat and Mass Transfer*, vol. 20, Apr., p. 323-330.
- Ries H., Spirk W. 1996. Nonimaging secondary concentrators for large rim angle parabolic troughs with tubular absorbers. *Applied Optics*, Vol. 35, Issue 13, pp. 2242-2245.
- Winston R., Benítez P., Miñano J.C. 2005. Non Imaging Optics. Elsevier Academic Press.
- Welford W. T., Winston R. 1989. High Collection Nonimaging Optics - Academic, New York.
- Heliotrough main dimensions, accessed Nov 25, 2015, <http://www.heliotrough.com>
- Ultimate Trough – Flabeg , accessed Nov 25, 2015, <http://www.flabeg-fe.com/en/engineering/ultimate-trough.html>

4. CHAPTER 4: OPTICAL ANALYSIS OF A TWO STAGE XX CONCENTRATOR FOR PARAMETRIC TROUGH PRIMARY AND TUBULAR ABSORBER WITH APPLICATION IN SOLAR THERMAL ENERGY (STE) TROUGH POWER PLANTS

This chapter will be published as a paper with the following authors and abstract:

Authors: **Juan Pablo Núñez Bootello**, email address: jp.nunez@abengoa.com
Abengoa. Calle Energía Solar, 1. Seville 41014, Spain

Henry Price, email address: hank.price@abengoa.com
Abengoa. 1250 Simms Street. Lakewood 80401, USA

Manuel Silva Pérez, email address: msilva@us.es
University of Seville. Group of Thermodynamics and Renewable Energy,
Department of Energy Engineering. Camino de Los Descubrimientos, s/n.
41092- Seville, Spain

Manuel Doblare Castellano, email address: manuel.doblare@abengoa.com
Abengoa. Calle Energía Solar, 1, Seville 41014, Spain.

Abstract:

A new symmetric Non Imaging Parametric Trough Collector for an evacuated circular receiver is proposed having an absorber radius of 70mm similar to the LS3 / Eurotrough absorber one, and a circular secondary. The optical design method is explained and a sensitivity analysis is conducted with respect to the diameter of the secondary and to the acceptance angle. In the design process, transmission, absorption and reflection losses are neglected. A secondary mirror radius of 145 mm and an acceptance angle of +/- 14 mrad were chosen as realistic values. For these values a concentrator geometry having 8.7 m gross aperture and 100% collection efficiency for rays impinging on the primary within the referred acceptance angle is obtained producing a net concentration ratio relative to the thermodynamic ideal limit of 0.52 compared to 0.31 for traditional Parabolic Trough Collectors. The new concentrator is composed of a primary discontinuous reflector with two symmetrical portions with parametric geometry, and a central parabolic portion located between the other two. The secondary concentrator can be manufactured by partially mirroring a diameter adapted glass tube - either internally or externally - or alternatively by means of a commercial evacuated receiver and an independent 145 mm radius arc of circumference external secondary reflector. Montecarlo ray tracing results show that only 15% of the rays undergo secondary reflection before arriving to the absorber and a sharp angle transmission curve. The new concentrator is proposed for application in STE trough power plants.

Keywords: Parabolic trough; Wind loads, SMS method; Non-imaging optics; Concentrated Solar Power, Solar Thermal Electric

References:

- Benitez P., García R., Miñano J.C. 1997. Contactless efficient two-stage solar concentrator for tubular absorber. *Appl Opt.* Oct 1;36(28):7119-24
- Cannavaro D., Chaves J., Collares M. 2013. New second-stage concentrators (XX SMS) for parabolic primaries; Comparison with conventional parabolic trough concentrators. *Solar Energy.* Volume 92, June, Pages 98–105
- Eberle Spencer Domina; Montgomery, L. L.; Fitzgerald, Joseph F. 1965. Macrofocal Conics as Reflector Contours. *Journal of the Optical Society of America*, vol. 55, issue 1, p.5
- Fernández-García, Zarza E., Valenzuela L., Pérez M. 2010. Parabolic-trough solar collectors and their applications. *Renewable and Sustainable Energy Reviews.* Volume 14, Issue 7, September, Pages 1695–1721
- Marcotte P., Manning K. 2013. Development of an advanced large-aperture parabolic trough collector. *Energy Procedia* Volume 49, 2014, Pages 145–154. Proceedings of the SolarPACES 2013 International Conference
- Pereira M.C., Gordon J.M., Rabl A., Winston R. 1991. High concentration two stage optics for Parabolic Trough Solar Collectors with tubular absorber and large rim angle. *Solar Energy.* Volume 47, Issue 6, Pages 457–466
- Rabl A. 1985. *Active Solar Collectors and Their Applications* - Oxford U. Press, Oxford, UK.
- Winston R., Benitez P., Miñano J.C. 2005. *Non Imaging Optics*. Elsevier Academic Press.

5. CHAPTER 5: PARABOLIC TROUGHS vs FRESNEL CONCENTRATORS

Parabolic troughs can get quite big and hard to handle, especially for large rim angles, those that yield the most compact concentrators. One way around this problem is to Fresnelize the mirror, that is, replace it by a set of small mirrors (heliostats) on a straight line, flats that mimic the optical behaviour of the parabolic mirror they replace. In Fresnel collectors a large number of small mirrors (called heliostats) move tracking the sun and keeping its light concentrated onto the receiver (Chaves J. et al., 2010).

One of the advantages of this technology is its simplicity and the possibility to use low cost components. Direct saturated steam systems with fixed absorber tubes have been operated without problems. This technology eliminates the need for HTF and heat exchangers. Increasing the efficiency depends on superheating the steam; however, this is still a challenge that has to be overcome. This technology is currently less deployed than the parabolic trough one. Concentration and temperature of the fluid in the solar field – to date mostly saturated steam – are lower than in the central receiver and parabolic trough technologies (Estela, 2012). From an optical point of view Fresnel concentrators may have important losses. If the heliostats are spaced from each other, some light will miss them and be lost. If the heliostats are close to each other, they will block part of each other's reflected light, also producing losses. Therefore, cosine losses are of high importance in this type of plants especially in the early morning and in the late evening and have to be carefully evaluated.

As signaled, it is out of the scope of this thesis to compare Fresnel concentrators with Parabolic or Parametric Trough concentrators at a plant level, but since both optics share the same concentration limit, a comparison in terms of concentration ratio relative to the maximum thermodynamic limit is done. It is the scope of this chapter to understand the optics of the different state of the art Fresnel collectors.

In any case the Etendue-matched two-stage concentrators with multiple receivers has the best optics in terms of concentration ratio relative to the maximum thermodynamic limit among all of current state of the art Fresnel solutions. The product efficiency times the concentration relative to maximum remains in the range 55% up to 85% which is higher than the 60% obtained with the PmTC developed in this thesis.

References:

- Chaves J., 2008. *Introduction to non imaging optics*. s.l.:CRC Press.
- Chaves J., C.-P. M., 2010. Etendue-matched two-stage concentrators with multiple receivers. *Solar Energy*, Volumen 84, p. 196–207.
- Collares M., 2009. *Etendue matched reflective fresnel concentrators*. Berlin, Proceedings 15th International SolarPaces Symposium, September 14-18.
- Friedman R.P., G. J. R. H., 1996. Compact high-flux twostage solar collectors based on tailored edge-ray concentrators.. *Solar Energy*, 56(6), p. 607–615.
- Gordon J.M., R. H., 1993. Tailored edge-ray concentrators as ideal second stages for Fresnel reflectors. *Applied Optics* 32, Issue 13, p. 2243–2251..
- Häberle A., Z. C. L. H. M. M. W. C. T. F. D. J., 2002. *TheSolarmundo line focussing Fresnel collector. Optical and thermal performance and cost calculations*. Zürich, International symposium on concentrated solar power and chemical energy technologies.
- Mills D.R., G. L., 2000. Compact linear Fresnel reflector solar thermal powerplants. *Solar Energy*, 68(3), pp. 263-283.
- Morin G., P. W. E. M. U. R. H. A. B. M., 2006. *Road map towards the demonstration of a linear Fresnel collector using single tube receiver*. Seville, 13th International Symposium on Concentrated Solar Power and Chemical Energy Technologies .
- Nuñez-Bootello J.P., O. R., 2010. *Fresnel type solar concentrator plant with an optimized secondary*. PCT, Patente nº WO 20101100293.
- Winston R., B. P. M. J., 2005. *Non Imaging Optics*. s.l.:Elsevier Academic Press.

6. CHAPTER 6: AERODYNAMICS OF NEW SOLAR PARAMETRIC TROUGHS: TWO DIMENSIONAL AND THREE DIEMENSIONAL SINGLE MODULE NUMERICAL ANALYSIS

This chapter will be published as a paper with the following authors and abstract:

Authors: **Juan Pablo Núñez Bootello**, email address: jp.nunez@abengoa.com
Abengoa. Calle Energía Solar, 1. Seville 41014, Spain

Monica de Mier Torrecillas, email address: monica.mier@abengoa.com
Abengoa. Calle Energía Solar, 1. Seville 41014, Spain

Manuel Dobláré Castellano, email address: manuel.doblare@abengoa.com
Abengoa. Calle Energía Solar, 1, Seville 41014, Spain.

Manuel Silva Pérez, email address: msilva@us.es
University of Seville. Group of Thermodynamics and Renewable Energy,
Department of Energy Engineering. Camino de Los Descubrimientos, s/n.
41092- Seville, Spain

Abstract:

Two new symmetric Non Imaging Parametric Trough Collectors (PmTC) for circular and flat evacuated receiver have been proposed with a potential improvement in the net concentration ratio relative to the thermodynamic ideal limit beyond 65% compared to commercial Parabolic Trough Collectors (PTC) while maintaining or increasing the rim angle. Both collectors are composed of a symmetrical parametric primary discontinuous reflector geometry and a secondary concentrator with potential to reduce the wind loads and effectively reduce the cost of the solar field. Computational Fluid Dynamics (CFD) has been used as a “virtual” wind tunnel to compare the flow around a single model-scale module of the two PmTCs and the two commercial LS2 and LS3 PTCs, in a range of pitch angles. Two case studies - 2D and 3D simulations - have been analyzed. Wind turbulence intensity was not taken into account. Velocity vector field, mean values of aerodynamic drag, lift and moment coefficients and flow patterns were computed. Results confirm that the PmTC for circular receiver behaves very similarly to the LS2 and LS3 geometries for the drag, lift and moment coefficients. The PmTC for flat absorber shows the worst performance showing more than 25% penalization in terms of maximum drag and moment values and more than 50% penalization in terms of maximum lift in comparison with the other three collectors. The 2D case study show worse coefficients when compared to the 3D case by a factor of 2. Analysis of averaged velocity vector field at mid-section show a smaller wake in the 3D case study for the four collectors and all pitch angles and a lower influence of the gap in the primary reflector. An

additional comparison of the LS2 three dimensional results with and without turbulence intensities - the latter results taken from an earlier work - show very good agreement for the mean lift and moment values and a 20% difference for the mean drag due to the fact that turbulence fluctuations over the mean velocity profile add more energy to the system. Further 3D CFD simulations with turbulence intensities for a complete solar field design are needed in order to evaluate the potential of both PmTC to effectively reduce the cost of the solar field

References

- Andre M., M.-T. M. W. R. B. K., 2014. *A comparative study of Finite element and lattice Boltzmann methods for estimation of dynamic wind loads*. Germany, Sixth International Symposium on Computational Wind Engineering (CWE2014).
- Andre M., M.-T. M. W. R. B. K., 2015. Numerical simulation of wind loads on parabolic trough solar collectors using lattice Boltzmann and finite element methods. *Journal of Wind Engineering and Industrial Aerody*, p. (in submission).
- CSP, 2015. *Concentrating Solar Power Projects*. [En línea]
Available at: <http://www.nrel.gov>
- Estela, 2012. *Solar Thermal Electricity – Strategic Research Agenda 2020 – 2025*, : European Solar Thermal. Electricity Association.
- EUROTROUGHII, 2003. *Final report Extension, Test and Qualification of EUROTROUGH from 4 to 6 Segments at Plataforma Solar de Almería*, s.l.: European Community.
- Fernández-García A., Z. E. V. L. P. M., 2010. Parabolic-trough solar collectors and their applications. *Renewable and Sustainable Energy Reviews*, Volume 14(Issue 7), p. 1695–1721.
- Giannuzzi G. M., M. C. E. M. A. S. V. A. N. D., 2007. Structural Design Criteria for Steel Components of Parabolic-Trough Solar Concentrators.. *J. Sol. Energy Eng*, Volumen 129, pp. 382-390.
- Hachicha A.A., R. I. C. J. O. A., 2013. Numerical simulation of wind flow around a parabolic trough solar collector. *Appl. Energ.*, 107(doi.10.1016), pp. 426-437.
- Hosoya N., P. J. G. R. K. D., 2008. *Wind Tunnel Tests of Parabolic Trough Solar Collectors*., National Renewable Energy Laboratory: Technical Report NREL/SR-550-32282..
- IEA, 2014. *Solar Thermal Electricity. Technology Roadmap – 2014 Edition*, : .
- Mann J., 1998. Win Field Simulation. *Probabilistic Engineering Mechanics*, vol 13(), pp. 269-282.
- Marcotte P., M. K., 2014. 2013. Development of an advanced large-aperture parabolic trough collector.. *Energy Procedia. Proceedings of the SolarPACES 2013 International Conference*, Volumen Volume 49, p. 145–154.
- Mier-Torrecilla M., H. E. D. M., 2014. *Numerical calculation of wind loads over solar collectors..* 163-173, Energy Procedia 49.

Naeeni N., Y. M., 2007. Analysis of wind flow around a parabolic collector fluid flow. *Renew. Energ.*, 32(doi.10.1016), pp. 1898-1916.

Paetzolda J., C. S. F. D. A., 2014. *Wind Engineering Analysis of Parabolic Trough Collectors to Optimise Wind Loads and Heat Loss*. Beijin, International Conference on Concentrating Solar Power and Chemical Energy Systems, SolarPACES 2014.

Peterka J.A., S. J. C. J., 1980. *Mean wind forces on parabolic-trough solar collectors*. Tech. Report SAND80-7023, s.l.: Sandia National Laboratories.

Winston R., B. P. M. J., 2005. *Non Imaging Optics*. s.l.:Elsevier Academic Press.

Xflow, 2015. *XFlow Computational Fluid Dynamics*. [En línea]

Available at: www.xflow-cfd.com

[Último acceso: 2015].

Zemler M.K., B. G. R. O. B. S., 2013. Numerical study of wind forces on parabolic solar collectors. *Renew. Energ.*, 60(doi.10.1016), pp. 498-505.

7. CHAPTER 7: PARAMETRIC TROUGH COLLECTOR (PmTC) FOR A COMMERCIAL EVACUATED RECEIVER: OPTICAL PERFORMANCE AND PLANT SIMULATIONS

This chapter will be published as a paper with the following authors, abstract and keywords:

Authors: **Juan Pablo Núñez Bootello**, email address: jp.nunez@abengoa.com
Abengoa. Calle Energía Solar, 1. Seville 41014, Spain

Markus Schramm, email address: markus.schramm@abengoa.com
Abengoa. Calle Energía Solar, 1. Seville 41014, Spain

Manuel Silva Pérez, email address: msilva@us.es
University of Seville. Group of Thermodynamics and Renewable Energy,
Department of Energy Engineering. Camino de Los Descubrimientos, s/n.
41092- Seville, Spain

Manuel Doblaré Castellano, email address: manuel.doblare@abengoa.com
Abengoa. Calle Energía Solar, 1, Seville 41014, Spain.

Abstract:

A new symmetric Non Imaging Parametric Trough Collector (PmTC) design for a commercial evacuated receiver having 8.12 m net aperture, 100% collection efficiency for an acceptance angle of +/- 14 mrad, and net concentration ratio relative to the thermodynamic ideal limit of 0.52 compared to 0.31 of traditional Parabolic Trough Collectors (PTC) is here presented. Since the collector was designed ignoring transmission, absorption and reflection optical losses, calculations of the optical efficiency by means of Montecarlo raytracing simulations using real slope errors distributions and taking into account Fresnel Losses was done. Comparison with a commercial Parabolic Trough Collector (PTC) shows an optical penalization of 5.1% due to the reflectivity and additional dirtiness of the secondary mirror, to an increase in the end losses and to the Fresnel losses. NREL System Advisor Model (SAM) was used to perform annual simulations of a commercial Solnova type 50 MWe oil PTC power plant without thermal energy storage located in Seville (Spain). A PTC solar field consisting on 90 loops, each one having 4 Solar Collector Assemblies (SCAs) with 150 m length was first modeled resulting in a gross production of 386 kWh/(m² year) in agreement with reported data. A PmTC solar field with the same module length and with similar collector area to the PTC one was also used for simulation. A final configuration of 94 loops and 4 Solar Collector Assemblies (SCAs) with 100 m length per loop yields a gross production of 379 kWh/(m² year) showing no improvement compared to the reference PTC plant.

Keywords: Parabolic trough; solar thermal power plant, non-imaging optics; concentrated solar power; optical efficiency

References

- International Energy Agency, 2014. Solar Thermal Electricity. Technology Roadmap – 2014 Edition, s.l.: IEA information paper.
- CSP World Map – CSP World, accessed Dec 10, 2015, <http://www.csp-world.com/cspworldmap>
- Estela, 2012. Solar Thermal Electricity – Strategic Research Agenda 2020 – 2025, : European Solar Thermal. Electricity Association.
- Nunez-Bootello J.P, Price H. Silva M., Doblaré M., 2016 (accepted for publication). Optical analysis of a two stage XX SMS concentrator for parametric trough primary and flat absorber with application in DSG solar thermal plants. ASME Journal of Solar Energy Engineering: Including Wind Energy and Building Energy Conservation
- Nunez-Bootello J.P, Price H. Silva M., Doblaré M., 2016 (under review). Optical analysis of a two stage XX concentrator for parametric trough primary and tubular absorber with application in STE trough power plants. ASME Journal of Solar Energy Engineering: Including Wind Energy and Building Energy Conservation
- Cannavaro D., Chaves J., Collares M. 2013. New second-stage concentrators (XX SMS) for parabolic primaries; Comparison with conventional parabolic trough concentrators. Solar Energy. Volume 92, June, Pages 98–105
- Wagner M.J., Gilman P., 2014, Technical Manual for the SAM Physical Trough Model
- Armenta-Deu C., 1991. A correlation model to compute the incidence angle modifier and to estimate its effect on collectible solar radiation. Renewable Energy Vol. I, No. 5/6, pp. 803-809.
- Ciemat, 2004. Plantas solares con colectores Cilindro Parabólicos, Almería: PSA
- Eurotrough II, 2003. Final report Extension, Test and Qualification of EUROTROUGH from 4 to 6 Segments at Plataforma Solar de Almería, s.l.: European Community
- Marcotte P., Manning K. 2013. Development of an advanced large-aperture parabolic trough collector. Energy Procedia Volume 49, 2014, Pages 145–154. Proceedings of the SolarPACES 2013 International Conference
- Abengoa presentation, accessed Dec 10, 2015,
http://energy.gov/sites/prod/files/2014/01/f7/csp_review_meeting_042513_price.pdf
- San Vicente G., 2009. Surface Modification of Porous Antireflective coatings for Solar Glass Covers.. Berlin, Germany, SolarPACES 2009 – Electricity, fuels and clean water powered by the sun.
- Burkholder F., 2009. Heat Loss Testing of Schott's 2008 PTR70 Parabolic Trough Receiver, U.S. Department of Energy: NREL.

Abengoa presentation, accessed Dec 10, 2015,
http://antiguo.minenergia.cl/minwww/export/sites/default/12_Utiles/banners/presentaciones/06_091006AbengoaSolar.pdf

Concentrating Solar Power Projects, accessed Dec 10, 2015, <http://www.nrel.gov>

Fernández-García, Zarza E., Valenzuela L., Pérez M. 2010. Parabolic-trough solar collectors and their applications. Renewable and Sustainable Energy Reviews. Volume 14, Issue 7, September, Pages 1695–1721

CONCLUSIONS

The main conclusions of the thesis are:

5. Two Parametric Trough Collectors for flat and for circular absorber geometries obtained using non-imaging optics are presented and discussed. The flat absorber solution can be replaced by a multi-tube receiver which has the advantage of a better heat transfer from the absorbing coating to the heat carrier fluid so that large number of tubes improves the thermal efficiency. As the pumping power increases almost as a cubic power of this number, Direct Steam Generation remains the best application for this kind of receiver. The circular absorber solution can be solved with a partially mirrored big glass tube hosting an eccentric absorber tube inside or by using a commercial evacuated receiver with an external secondary. In this case either oil, molten salt or water can be used as heat transfer fluids.
6. A comparison in terms of concentration ratio relative to the maximum thermodynamic limit with state of the art trough collector based on a parabolic shape and with state of the art Fresnel collectors was done. The first comparison shows that the ratio concentration relative to the thermodynamic maximum increases up to 90% maintaining rim angles greater than 80° with the same effective acceptance angle than current LS3 / Eurotrough optics. Thus both proposals have the potential to deliver considerably more energy onto the same absorber perimeter for the same effective acceptance angle. In addition the shape of the proposed collectors having important discontinuities in the middle of the primary reflectors were identified as opportunities to reduce wind loads while adding flexibility to control the separation between the ensemble receiver-secondary mirror support substructure and the concentrator torque structure.

On the other hand, the etendue-matched two-stage Fresnel concentrator with multiple receivers has a product efficiency times the concentration relative to maximum in the range 55% up to 85% which is higher than the 60% one obtained with the best PmTC solution developed in this thesis. This second comparison is performed only from an optical point of view since both optics share the same concentration limit but it is out of the scope of this thesis to compare Fresnel concentrators with Parabolic or Parametric Trough concentrators at a plant level.

7. Detailed Computational Fluid Dynamics (CFD) wind tunnel simulations used to compare the flow around a single model-scale module of the two proposed concentrators and the LS3 / Eurotrough parabolic trough in a range of pitch angles, confirm that the solution for circular receiver behaves very similarly to the LS3 / Eurotrough geometry for the drag, lift

and moment coefficients and that the solution for flat absorber shows more than 25% penalization in terms of maximum drag and moment values and more than 50% penalization in terms of maximum lift. This results together with the fact that in the flat receiver collector all rays suffer two reflections before reaching the absorber while only 15% of the rays undergo secondary reflection before arriving to the absorber in the case of the circular receiver solution, and the fact that it does not exist a supplier with a commercial solution for the multitubular receiver have motivated the selection of the solution for circular receiver with commercial evacuated receiver an external secondary as the option to be evaluated at plant level.

8. To understand the potential of the selected solution compared to the parabolic baseline two commercial 50 MWe oil parabolic trough power plant model without thermal energy storage located in Seville (Spain) models were built up. In the case of the parametric concentrator the collector area was chosen similar to the area of the parabolic collector to assure similar single loop mass flow rates. Since the hypothesis of zero transmission, absorption and reflection optical losses was made in the design process calculations, optical efficiency calculations using real slope errors distributions by means of Montecarlo raytracing simulations considering Fresnel losses were performed. Contrary to initial expectations, comparison with commercial Parabolic Trough Collector shows an optical penalization at zero solar incidence of 5.1% due to the reflectivity and additional dirtiness of the secondary mirror, to an increase in the end losses and to the Fresnel losses. Annual simulations show a 2.5% reduction in electricity yield when compared to the reference PTC plant. The improvement relative to the optical performance is due in part to lower thermal losses. Thus, the proposed solution does not show improvement compared to the reference PTC plant for a design loop oil outlet temperature of 391°C.

Main contributions

The main contributions of this work are:

1. A review of parabolic trough and Fresnel collectors' optics is done.
2. A new trough collector for direct steam generation is proposed. Its design method and the final geometry boundary conditions are explained.
3. A new trough collector with evacuated circular receiver with application in STE trough power plants is proposed. Its design method and the final geometry boundary conditions are also explained. A sensitivity analysis of the shape is done with respect to the acceptance angle of the collector and the geometry of the secondary concentrator for a fixed commercial absorber diameter.
4. Both new parametric trough designs are compared from an optical point of view with the LS3 / Eurotrough parabolic trough and with state of the art Fresnel collectors.
5. 2D and 3D CFD simulations as a "virtual" wind tunnel were performed to compute the flow around a single model-scale. Further comparisons of the two proposed collectors with the LS2 and LS3 PTCs in terms of drag, lift and moment mean values were done.
6. Two 50 MWe oil parabolic trough power plant models without thermal energy storage were build up, one with conventional Parabolic Trough Collector and other with the proposed Parametric Trough Collector for commercial circular receiver and external secondary. Comparisons from an efficiency and an electricity production point of view were performed.

Future Work

Future work recommendations are:

1. Conduct 3D CFD simulations taking into account turbulence intensities for the whole solar field to obtain mean and RMS lift, drag and moments values with the aim of identifying wind loads for the design for strength of the structures and the collectors drive mechanisms.
2. Proceed to design a structure for the proposed PmTCs taking into account operational conditions and design requirements (safety, optical performance and mechanical functionality).
3. Conduct techno economic analyses, with and without thermal storage, including real cost data in order to project results in terms of Levelized Cost of Electricity (LCoE) and not only in terms of efficiency and electricity yield.
4. Make further studies using molten salt as heat transfer with both higher fluid and cycle temperatures in order to understand how the new concentration ratio affects thermal losses, global efficiency and LCoE as a function of the working temperature.
5. Investigate in new anidolic design methods and trough geometries allowing the control of Fresnel Losses for STE commercial evacuated receivers.

8. ANNEX 1: COMMENTS ON THE CONVERSION OF ENCLOSED BLACKBODY RADIATION

In Chapter 1 it was reported Petela's results on the exergy of isotropic blackbody radiation by considering the deformable reflective enclosure of Figure 1-9 Enclosure with perfectly reflecting internal surfaces (Bejan A., 2006). But two questions arise with this approach (Bejan A., 2006):

What is the origin of the equilibrium blackbody radiation system (V_1, T_1)?

What is the ultimate fate of the blackbody radiation of temperature T_2 left when the system reaches its dead state?

If we analyze the system from a more global point of view (see Figure 8-1 Reversible cycle executed by an enclosed radiation system in communication with two temperature reservoirs (Bejan A., 2006))

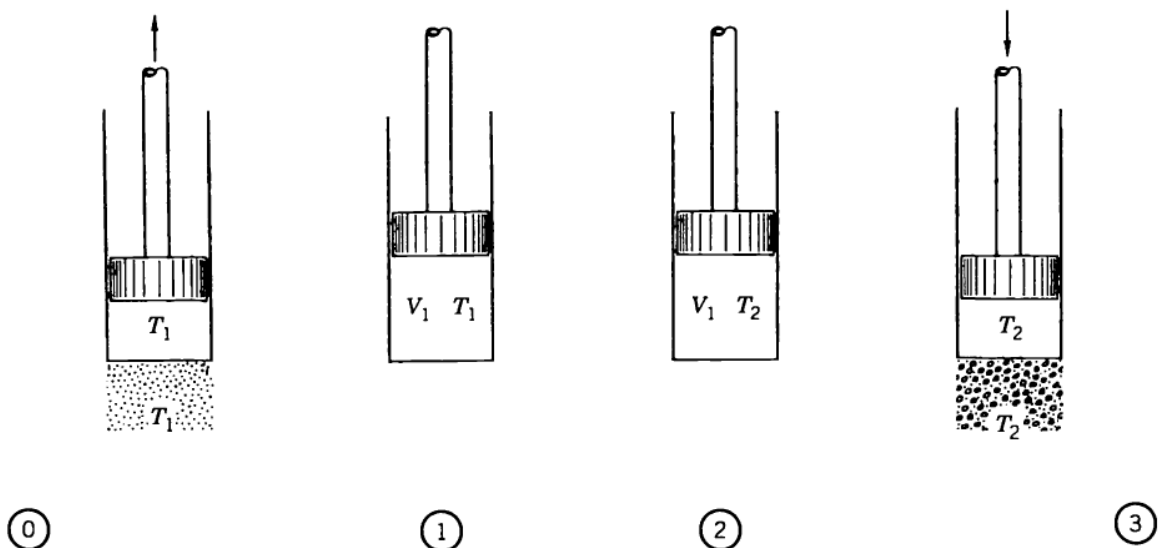


Figure 8-1 Reversible cycle executed by an enclosed radiation system in communication with two temperature reservoirs (Bejan A., 2006)

The first process, $0 \rightarrow 1$, accounts for the reversible manufacture of the (P_1, V_1) radiation system while in thermal contact with temperature reservoir T_1 . The system volume increases from zero to V_1 as reservoir T_1 heats the system isothermally and as the system performs the reversible work.

$$W_{0-1,rev} = \frac{1}{3}U_1V_1 \quad (\text{Annex 1.1})$$

The heat extracted from reservoir T_1 is:

$$Q_{0-1,rev} = \frac{4}{3}U_1V_1 \quad (\text{Annex 1.2})$$

The last process $2 \rightarrow 3$ runs in the reverse direction than this one

Putting the three results together: $0 \rightarrow 1 \rightarrow 2 \rightarrow 3$ one can obtain:

$$\oint \delta W = W_{0-1,rev} + W_{1-2,rev} + W_{2-3,rev} = \frac{4}{3}U_1V_1 - \frac{4}{3}U_2V_2 = \frac{4}{3}U_1V_1 \left(1 - \frac{T_2}{T_1}\right) \quad (\text{Annex 1.3})$$

using:

$$U_2 = aT_2^4 = aT_1^4 \frac{T_2^4}{T_1^4} = U_1 \frac{T_2^4}{T_1^4} \quad (\text{Annex 1.4})$$

$$V_2 = V_1 \left(\frac{T_1}{T_2}\right)^3 \quad (\text{Annex 1.5})$$

Dividing this network output by the heat supplied by the high temperature reservoir we get the expected Carnot Cycle efficiency:

$$\eta_C = 1 - \frac{T_2}{T_1} \quad (\text{Annex 1.6})$$

This result is expected because the efficiency of a reversible cycle executed by a closed system while in communication with two heat reservoirs is independent of the nature of the fluid employed by the engine (Bejan A., 2006).

If we replace the reversible expansion process $0 \rightarrow 1$ with a spontaneous irreversible process in which the system does not deliver any work to the assumed external mechanism (we label this new process as $0 \rightarrow 1$ zero work). Physically this new process begins with a completely evacuated enclosure of volume V_1 , which is placed suddenly in thermal communication with reservoir T_1 (Bejan A., 2006).

In this case:

$$W_{0-1,zero-work} = 0 \quad (\text{Annex 1.7})$$

$$Q_{0-1,zero-work} = U_1V_1 \quad (\text{Annex 1.8})$$

$$\oint \delta W = W_{1-2,rev} + W_{2-3,rev} = U_1 V_1 - \frac{4}{3} U_2 V_2 = U_1 V_1 \left(1 - \frac{4}{3} \frac{T_2}{T_1} \right) \quad (\text{Annex 1.9})$$

Dividing this network output by the heat supplied by the high temperature reservoir one obtains the Spanner's efficiency

$$\eta_s = 1 - \frac{4}{3} \frac{T_2}{T_1} \quad (\text{Annex 1.10})$$

Which is the maximum heat-engine efficiency for the class of cycles where the filling of the cylinder and piston apparatus occurs spontaneously (irreversibly) without the possibility of delivering useful work.

9. ANNEXE 2: PTC DEVELOPMENTS IN ABENGOA IN THE LAST 15 YEARS

During the last 15 years Abengoa has designed, developed, prototyped and marketed a set of different collectors:

- i) The Eurotrough Collector developed from 1998 to 2003 under a consortium of European companies. It has a rectangular torque-box support structure with hot rolled profiles holding the support arms for the parabolic mirror facets (Abengoa presentation, 2013) and (Fernández-García A., 2010).



Figure 9-1 Eurotrough Collector

- ii) The Astro Collector developed in 2007 is a torque box design evolution of the Eurotrough concept that uses low cost steel profiles with no welded frames and with optimized factory assembly allowing the reduction of labour for assembly (Abengoa presentation, 2013).



Figure 9-2 Abengoa Astro Collector

- iii) The Phoenix Collector developed in 2009 hosts the same parabola than Astro and Eurotrough but is composed of an extruded aluminium space frame designed for rapid module assembly with no need of alignment jig.



Figure 9-3 Abengoa Phoenix Gen 2.0 Collector

iv) The E2 Collector developed in 2011 is the steel spaceframe variation of the Phoenix design. It has new crimped steel members and hubs, the Astro torque transfer connection and requires jig for alignment (Abengoa presentation, 2013)



Figure 9-4 Abengoa E 2 Collector

v) The SpaceTube (Marcotte P., 2014) and (Abengoa presentation, 2013) developed in 2013 is a new cost-optimized parabolic trough collector with an aperture width greater than 8m based on a helical steel space frame structure layout hybridizing a torque tube and a space frame to capture the most desirable aspects of each.



Figure 9-5 Abengoa Spacetube Collector

All these developments have been internally and externally certified in terms of geometrical properties and quality parameters by means of photogrammetry and deflectometry measurements. From this experience a database of real slope errors has been created.

REFERENCES

- Abengoa presentation, 2009. *Ministerio de Energía - Gobierno de Chile*. [En línea] Available at:
http://antiguo.minenergia.cl/minwww/export/sites/default/12_Utiles/banners/presentaciones/06_091006AbengoaSolar.pdf
[Último acceso: 10 Dec 2015].
- Abengoa presentation, 2013. *Department of Energy*. [En línea] Available at:
http://energy.gov/sites/prod/files/2014/01/f7/csp_review_meeting_042513_price.pdf
[Último acceso: 10 Dec 2015].
- Andre M., M.-T. M. W. R. B. K., 2014. *A comparative study of Finite element and lattice Boltzmann methods for estimation of dynamic wind loads*. Germany, Sixth International Symposium on Computational Wind Engineering (CWE2014).
- Andre M., M.-T. M. W. R. B. K., 2015. Numerical simulation of wind loads on parabolic trough solar collectors using lattice Boltzmann and finite element methods. *Journal of Wind Engineering and Industrial Aerody*, p. (in submission).
- Armenta-Deu C., 1991. A correlation model to compute the incidence angle modifier and to estimate its effect on collectible solar radiation. Vol. I. *Renewable Energy*, 1(5), pp. 803-809.
- Bejan A., 2006. *Advanced Engineering Thermodynamics*. Third Edition ed. Durham: Wiley.
- Benitez P., G. R. M. J., 1997. Contactless efficient two-stage solar concentrator for tubular absorber. *Appl Opt*, Volumen Oct 1;36(28):7119-24.
- Benítez P., M. J. Z. P. M. R. C. A. B. M. C. J. H. M., 2010. High performance Fresnel-based photovoltaic concentrator. *Optics Express*, 18(51), pp. A25-A40.
- Burkholder F., K. C., 2009. *Heat Loss Testing of Schott's 2008 PTR70 Parabolic Trough Receiver*, U.S. Department of Energy: NREL.
- Cannavaro D., C. J. C. M., 2013. New second-stage concentrators (XX SMS) for parabolic primaries; Comparison with conventional parabolic trough concentrators.. *Solar Energy*, Volumen Volume 92, June, p. 98–105.
- Chaves J., 2008. *Introduction to non imaging optics*. s.l.:CRC Press.
- Chaves J., C.-P. M., 2010. Etendue-matched two-stage concentrators with multiple receivers. *Solar Energy*, Volumen 84, p. 196–207.
- Chaves J., C. P. M., 2010. Etendue matched two stage concentrators with multiple receivers. *Solar Energy*, Volume 84(Issue 2), p. 196–207.
- Ciemat, 1990 - 1994. *ARDIIS Receiver Second stage concentrator design, construction and evaluation.*, s.l.: EU Joule II Programme Ardiss Project - Contract No: JOU2 - CT94 – 0311.
- Ciemat, 2004. *Plantas solares con colectores Cilindro Parabólicos*, Almería: PSA.
- Collares M., 2009. *Etendue matched reflective fresnel concentrators*. Berlin, Proceedings 15th International SolarPaces Symposium, September 14-18.

Collares M., G. J. R. A. W. R., 1991. High concentration two stage optics for Parabolic Trough Solar Collectors with tubular absorber and large rim angle. *Solar Energy*, Volume 47(Issue 6), p. 457–466.

CSP, 2015. *Concentrating Solar Power Projects*. [En línea]
Available at: <http://www.nrel.gov>

Davies P. A., 1994. The edge ray principle of nonimaging optics. *JOSA A*, Volumen Vol. 11, Issue 4, pp. 1256-1259.

De Vos A., L. P. T. P. J. E., 1993. Entropy fluxes, endoreversibility, and solar energy conversion. *J. Appl. Phys.*, 74(3631).

Domina, E. S., Montgomery, L. L. & Fitzgerald, J. F., 1965. Journal of the Optical Society of America. *Macrofocal Conics as Reflector Contours*, vol. 55(issue 1), p. 5.

Duffie J.A., B. W. A., 1980. *Solar Engineering of Thermal Processes*. s.l.:Wiley.

Eberle D.S., M. L. L. F. J. F., 1965. Macrofocal Conics as Reflector Contours. *Journal of the Optical Society of America*, 55(1), p. 55.

Estela, 2012. *Solar Thermal Electricity – Strategic Research Agenda 2020 – 2025*, : European Solar Thermal. Electricity Association.

EurotroughII, 2003. *Final report Extension, Test and Qualification of EUROTROUGH from 4 to 6 Segments at Plataforma Solar de Almería*, s.l.: European Community.

Fernández-García A., Z. E. V. L. P. M., 2010. Parabolic-trough solar collectors and their applications. *Renewable and Sustainable Energy Reviews*, Volume 14(Issue 7), p. 1695–1721.

Flabeg, 2015. *Ultimate Trough*. [En línea]
Available at: <http://www.flabeg-fe.com/en/engineering/ultimate-trough.html>
[Último acceso: 25 Nov 2015].

Flagsol, 2015. *Heliotrough main dimensions*. [En línea]
Available at: <http://www.heliotrough.com>
[Último acceso: 25 Nov 2015].

Friedman R.P., G. J. R. H., 1996. Compact high-flux twostage solar collectors based on tailored edge-ray concentrators.. *Solar Energy*, 56(6), p. 607–615.

Giannuzzi G. M., M. C. E. M. A. S. V. A. N. D., 2007. Structural Design Criteria for Steel Components of Parabolic-Trough Solar Concentrators.. *J. Sol. Energy Eng*, Volumen 129, pp. 382-390.

Gordon J.M., R. H., 1993. Tailored edge-ray concentrators as ideal second stages for Fresnel reflectors. *Applied Optics* 32, Issue 13, p. 2243–2251..

Häberle A., Z. C. L. H. M. M. W. C. T. F. D. J., 2002. *TheSolarmundo line focussing Fresnel collector. Optical and thermal performance and cost calculations*. Zürich, International symposium on concentrated solar power and chemical energy technologies.

Hachicha A.A., R. I. C. J. O. A., 2013. Numerical simulation of wind flow around a parabolic trough solar collector. *Appl. Energ.*, 107(doi.10.1016), pp. 426-437.

Hosoya N., P. J. G. R. K. D., 2008. *Wind Tunnel Tests of Parabolic Trough Solar Collectors*., National Renewable Energy Laboratory: Technical Report NREL/SR-550-32282..

- Incropera F.P., D. D. B. T. L. A., 2007. *Fundamentals of Heat and Mass transfer*. 6th edition ed. s.l.:Wiley.
- International Energy Agency, 2007. *Contribution of renewables to energy security*, s.l.: IEA information paper.
- International Energy Agency, 2014. *Solar Thermal Electricity. Technology Roadmap – 2014 Edition*, s.l.: IEA information paper.
- Kabelac S., 2008. *Thermodynamic basics of solar radiation*. The Netherlands, 5th European Thermal-Sciences Conference.
- Landau D.P., B. K., 2005. *A Guide to Monte Carlo Simulations in Statistical Physics*. Second Edition ed. Cambridge: Cambridge University Press.
- Landsberg P. T, ., T. G., 1979. Thermodynamics of the conversion of diluted radiation. *Journal of Physics A - Mathematical and General*, Volumen 12, pp. 551-562.
- Landsberg P. T., T. G., 1980. Thermodynamic energy conversion efficiencies. *Journal of Applied Physics*, 51(7), p. .
- Landsberg P.T., 1959. The Entropy of a Non-Equilibrium Ideal Quantum Gas. *Proceedings of the Physical Society*, 74(4).
- Landsberg P.T., B. P., 1989. The thermodynamics of the conversion of radiation energy for photovoltaics. *Journal of Physics A: Mathematical and General*, Volume 22(Number 11).
- Leland T W. Jr, 2015. *Basic Principles of Classical and Statistical Thermodynamics*. [En línea] Available at: <http://trl.lab.uic.edu/1.OnlineMaterials/BasicPrinciplesByTWLeland.pdf>
- Lighting Research Center, 1990. *Illumination Fundamentals*, Rensselaer Polytechnic Institute: Optical Research Associates.
- Lüpfer E., G. M. S. W. E. A. O. R. Z. E. N. P., 2001. *Eurotrough design issues and prototype testing at PSA*. Washington, DC, proceedings of Solar Forum 2001 Solar Energy: The Power to Choose April 21-25.
- Mann J., 1998. Win Field Simulation. *Probabilistic Engineering Mechanics*, vol 13(), pp. 269-282.
- Marcotte P., M. K., 2014. 2013. Development of an advanced large-aperture parabolic trough collector.. *Energy Procedia. Proceedings of the SolarPACES 2013 International Conference*, Volumen Volume 49, p. 145–154.
- Martinez-Val J., A. A. A. R. M. J. V. M. R. A. R. A. M. M., 2011. Thermal performance analysis of linear receivers.. *Proceedings of the SolarPACES 2011 International Conference*, p. 489–498.
- Mier-Torrecilla M., H. E. D. M., 2014. *Numerical calculation of wind loads over solar collectors..* 163-173, Energy Procedia 49.
- Mills D.R., G. L., 2000. Compact linear Fresnel reflector solar thermal powerplants. *Solar Energy*, 68(3), pp. 263-283.
- Minano J.C., G. J., 1992. New method of design of nonimaging concentrators. *Applied Optics*, Vol. 31(Issue 16), pp. 3051-3060.

- Morin G., P. W. E. M. U. R. H. A. B. M., 2006. *Road map towards the demonstration of a linear Fresnel collector using single tube receiver*. Seville, 13th International Symposium on Concentrated Solar Power and Chemical Energy Technologies .
- Muñoz J., M.-V. J. R. A., 2011. Thermal regimes in solar-thermal linear collectors. *Solar Energy*, 85(5), p. 857.870.
- Naeeni N., Y. M., 2007. Analysis of wind flow around a parabolic collector fluid flow. *Renew. Energ.*, 32(doi.10.1016), pp. 1898-1916.
- NREL, 2015. *Concentrating Solar Power Projects*. [En línea] Available at: <http://www.nrel.gov> [Último acceso: 10 Dec 2015].
- Nunez-Bootello J.P., P. H. S. P. M. D. M., 2016 ((under review). Optical analysis of a two stage XX concentrator for parametric trough primary and tubular absorber with application in STE trough solar plants. *ASME Solar Energy Engineering: Including Wind Energy and Building Energy Conservation*.
- Nunez-Bootello J.P, P. H. S. M. D. M., 2016. Optical analysis of a two stage XX SMS concentrator for parametric trough primary and flat absorber with application in DSG solar thermal plants. *ASME Solar Energy Engineering: Including Wind Energy and Building Energy Conservation*, p. accepted for publication.
- Nuñez-Bootello J.P., O. R., 2010. *Fresnel type solar concentrator plant with an optimized secondary*. PCT, Patente nº WO 20101100293.
- Paetzolda J., C. S. F. D. A., 2014. *Wind Engineering Analysis of Parabolic Trough Collectors to Optimise Wind Loads and Heat Loss*. Beijin, International Conference on Concentrating Solar Power and Chemical Energy Systems, SolarPACES 2014.
- Peterka J.A., S. J. C. J., 1980. *Mean wind forces on parabolic-trough solar collectors*. Tech. Report SAND80-7023, s.l.: Sandia National Laboratories.
- Planck M., 1914. *The Theory of Heat Radiation*. NY: Dover Publications.
- Price H., L. E. K. D. Z. E. C. G. G. R. M. R., 2002. Advances in Parabolic Trough Solar Power Technology. *J. Sol. Energy Eng.*, 124((2)), pp. 109-125.
- Rabl A., 1977. Radiation transfer trough specular passages – a simple approximation. *International Journal of Heat and Mass Transfer*, Volumen vol. 20, pp. 323-330.
- Rabl A., 1985. *Active Solar Collectors and Their Applications*. s.l.:Oxford U. Press, Oxford, U.
- Rabl A., B. P. W., 1982. Optimization of parabolic trough solar collectors. *Solar Energy*, Vol. 29(No. 5), pp. 407-417.
- Ries H., S. W., 1996. Nonimaging secondary concentrators for large rim angle parabolic troughs with tubular absorbers. *Applied Optics*, Vol. 35(Issue 13), pp. 2242-2245.
- Ross R.T., 1967. Some Thermodynamics of Photochemical Systems. *J. Chem. Phys.*, 46(4590).
- San Vicente G., B. R. G. N. A., 2009. *Surface Modification of Porous Antireflective coatings for Solar Glass Covers..* Berlin, Germany, SolarPACES 2009 – Electricity, fuels and clean water powered by the sun.
- Sen Z., 2008. *Solar Energy Fundamentals and Modeling Techniques*. s.l.:Springer.

- Träger F. (Ed.), 2007. *Springer Handbook of Lasers and Optics*. Kassel - Germany: Springer.
- Wagner M. J., G. P., 2012. *Technical Manual for the SAM Physical Trough Model*, NREL: U.S. Department of Energy.
- Webb R.H., 1997. *Elementary Wave Optics*. Mineola, New York: Dover Publications Inc.
- Welford W. T., W. R., 1989. *High Collection Nonimaging Optics*. s.l.:Academic, New York.
- Winston R., B. P. M. J., 2005. *Non Imaging Optics*. s.l.:Elsevier Academic Press.
- Wright S., 1998. *Developments on the Entropy of Solar Radiation*, Canada: University of Victoria.
- Wright S., 2007. Comparative Analysis of the Entropy of Radiative Heat Transfer and Heat Conduction. *International Journal of Thermodynamics*, 10(1), pp. 27-35.
- Wright S., S. D. H. J. R. M., 2001. On the Entropy of radiative heat transfer in engineering thermodynamics. *International Journal of Engineering Science*, 39(15), pp. 1691-1706.
- Xflow, 2015. *XFlow Computational Fluid Dynamics*. [En línea]
Available at: www.xflow-cfd.com
[Último acceso: 2015].
- Zarza E., 2004. *Generación directa de vapor con colectores solares cilindro parabólicos - Proyecto DIrect Solar Steam (DISS)*, Madrid: CIEMAT.
- Zeghbrouk B.V., 2011. *Principles Of Semiconductor Devices*. s.l.:Prentice Hall.
- Zemler M.K., B. G. R. O. B. S., 2013. Numerical study of wind forces on parabolic solar collectors. *Renew. Energ.*, 60(doi.10.1016), pp. 498-505.